Brain (1997), **120,** 1173–1197

Regional cerebral blood flow throughout the sleep–wake cycle
An $H_2{}^{15}O$ PET study

A. R. Braun,[1] T. J. Balkin,[3] N. J. Wesensten,[3] R. E. Carson,[2] M. Varga,[1] P. Baldwin,[2] S. Selbie,[1] G. Belenky[3] and P. Herscovitch[2]

[1]*Language Section, Voice Speech and Language Branch, National Institute on Deafness and Other Communication Disorders,* [2]*PET Imaging Section, Clinical Center, National Institutes of Health, Bethesda,* [3]*Department of Behavioral Biology, Division of Neuropsychiatry, Walter Reed Army Institute of Research, Washington, USA*

Correspondence to: A. R. Braun, MD, Language Section, Voice Speech and Language Branch, National Institute on Deafness and Other Communication Disorders, Building 10, Room 5N118A, National Institutes of Health, Bethesda, MD 20892, USA

Summary

*To assess dynamic changes in brain function throughout the sleep–wake cycle, CBF was measured with $H_2{}^{15}O$ and PET in 37 normal male volunteers: (i) while awake prior to sleep onset; (ii) during Stage 3–4 sleep, i.e. slow wave sleep (SWS); (iii) during rapid eye movement (REM) sleep; and (iv) upon waking following recovery sleep. Subjects were monitored polysomnographically and PET images were acquired throughout the course of a single night. Stage-specific contrasts were performed using statistical parametric mapping. Data were analysed in repeated measures fashion, examining within-subject differences between stages [pre-sleep wakefulness–SWS (*n *= 20 subjects); SWS–post-sleep wakefulness (*n *= 14); SWS–REM sleep (*n *= 7); pre-sleep wakefulness–REM sleep (*n *= 8); REM sleep–post-sleep wakefulness (*n *= 7); pre-sleep wakefulness–post-sleep wakefulness (*n *= 20)]. State-dependent changes in the activity of centrencephalic regions, including the brainstem, thalamus and basal forebrain (profound deactivations during SWS and reactivations during REM sleep) are consistent with the idea that these areas are constituents of brain systems which mediate arousal. Shifts in the level of activity of the striatum suggested that the basal ganglia might be more integrally involved in the orchestration of the sleep–wake cycle than previously thought. State-dependent changes in the activity of limbic and paralimbic areas, including the insula, cingulate and mesial temporal cortices, paralleled those observed in centrencephalic structures during both REM sleep and SWS. A functional dissociation between activity in higher order, heteromodal association cortices in the frontal and parietal lobes and unimodal sensory areas of the occipital and temporal lobes appeared to be characteristic of both SWS and REM sleep. SWS was associated with selective deactivation of the heteromodal association areas, while activity in primary and secondary sensory cortices was preserved. SWS may not, as previously thought, represent a generalized decrease in neuronal activity. On the other hand, REM sleep was characterized by selective activation of certain post-rolandic sensory cortices, while activity in the frontoparietal association cortices remained depressed. REM sleep may be characterized by activation of widespread areas of the brain, including the centrencephalic, paralimbic and unimodal sensory regions, with the specific exclusion of areas which normally participate in the highest order analysis and integration of neural information. Deactivation of the heteromodal association areas (the orbital, dorsolateral prefrontal and inferior parietal cortices) constitutes the single feature common to both non-REM and REM sleep states, and may be a defining characteristic of sleep itself. The stages of sleep could also be distinguished by characteristic differences in the relationships between the basal ganglia, thalamic nuclei and neocortical regions of interest.*

Keywords: REM sleep; non-REM sleep; slow wave sleep; rCBF; PET

Abbreviations: ANCOVA = analysis of covariance; ANOVA = analysis of variance; EOG = electro-oculography; rCBF = regional CBF; ΔrCBF = change in rCBF; REM = rapid eye movement (sleep); SPECT = single photon emission computed tomography; SPM = statistical parametric mapping; SWS = slow wave sleep

Introduction

Despite a century of research, the fundamental changes that occur within the human brain during sleep remain a mystery. Animal studies have generated a wealth of data concerning the activity of deep brain and cortical structures during the sleep–wake cycle through the use of invasive techniques such as microelectrode stimulation, or recording and cannulation of discrete anatomic nuclei (Parmeggiani *et al*., 1985). However, because the use of microinvasive techniques limits the available sample space, a global picture of regional interrelationships within the brain has failed to emerge. In addition, the results of such studies may be species specific and their relevance to human sleep is therefore uncertain.

The modern study of sleep in human subjects began with the introduction of the surface EEG. This non-invasive technique, along with EMG and electro-oculography (EOG), has been used to define and study the various stages of sleep (Rechtschaffen and Kales, 1968). However, the relationship between EEG patterns recorded at the scalp and functional activity within cortical and subcortical structures remains unclear.

PET is a non-invasive technique which yields information about functional activity within all regions of the brain simultaneously, and thus constitutes an excellent means of studying sleep. The non-invasive nature of the method allows direct investigation of metabolic or biochemical processes which might be unique to the human brain, and permits simultaneous visualization and quantification of functional activity in individual regions of the cortex, subcortical structures and brainstem, across the sleep–wake cycle.

Sleep studies have been carried out using the FDG (2-fluoro-2-deoxyglucose)-PET method (Heiss *et al*., 1985; Buchsbaum *et al*., 1989; Hong *et al*., 1995), but this technique necessitates the integration of data collected over a period of 30 min or longer, and is therefore not ideal for independently characterizing the shorter-lived sleep stages. Likewise, studies using single photon emission computed tomography (SPECT) blood-flow agents (Madsen *et al*., 1991*a*; Asenbaum *et al*., 1995), are not ideal either. Although it is possible to segment individual sleep stages more accurately with certain SPECT blood-flow agents, their longer half-lives do not readily permit multiple studies of different sleep stages throughout a single scanning session.

In contrast, the $H_2{}^{15}O$-PET method represents the best technical approach currently available. Acquisition times are brief, making it possible to visualize functional brain activity during discrete sleep stages. In addition, the 123-s half-life of ^{15}O makes it possible to study multiple sleep stages in the same individual during a single night. We therefore used this method to identify the regional CBF (rCBF) patterns that are specifically associated with rapid eye movement (REM) sleep, non-REM sleep, and pre- and post-sleep wakefulness in normal volunteers, with each subject serving as their own control.

Methods

Subjects

This study was conducted using a protocol approved by the NIH NINDS review board. Informed consent was obtained from all subjects, according to the declaration of Helsinki, after the potential risks, hazards and discomfort associated with the study were explained. Subjects included 37 healthy male volunteers, 24.5 $\pm$ 3.1 years of age (mean $\pm$ SD, range 20 –32 years). Thirty-three were right-handed; the other four were left-handed, or performed skilled manual functions with either hand. All subjects, on the basis of history, physical examination and baseline laboratory evaluation were judged to be free of medical, neurological and psychiatric illnesses which might affect brain function. Subjects with a history of sleep disorders, or who had used prescription medications within 1 month prior to the PET procedure, were excluded from the study.

Sleep deprivation schedules

All subjects underwent sleep-deprivation or sleep-restriction procedures prior to the PET studies. Twelve subjects were scanned in the daytime, following 24–54 h of total sleep deprivation. Twenty-five subjects were scanned at night. One was studied following 43 h of total sleep deprivation, and the remaining 24 underwent the following sleep–wakefulness regimen: on Day 1, 8 h of sleep (23.00–07.00 hours) with selective REM sleep deprivation (brief wakings initiated at the first sign of REM sleep); on Day 2, 2 h of sleep (01.00–03.00 hours) with REM sleep deprivation; on Day 3: between 16 and 24 h of continuous wakefulness prior to the night-time PET study. To verify the absence of sleep during the sleep deprivation portions of the study, ambulatory polysomnographic recordings (EEG from C_3 and C_4, EMG and EOG) were made using Oxford Medilog 9000 recorders. For on-line monitoring during REM sleep deprivation procedures, polysomnographic signals from the Oxford recorders were routed through a Nihon Kohden electro-encephalograph (Model EEG-4317B).

Polysomnographic monitoring

Following the sleep deprivation period, subjects were positioned in the PET scanner and polysomnographically monitored (Grass Model 8–10D polygraph) for the duration of the study, with electrode placements at C_3 and C_4 sites, the outer canthus of each eye, and the submentalis muscle. Subjects' eyes were patched, and head motion was restricted during the scans by the use of a thermoplastic mask fitted to each subject's head and attached to the scanner bed. Subjects

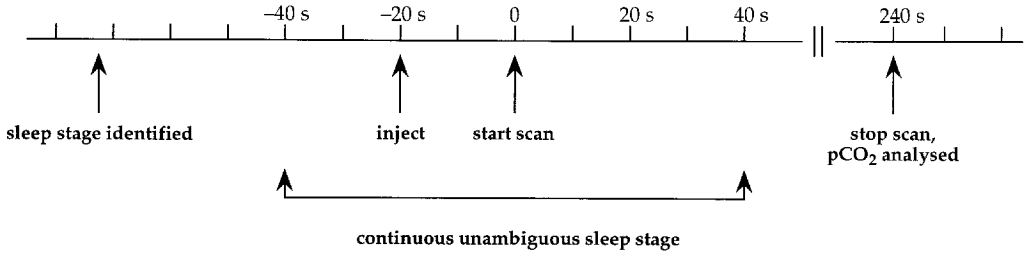

Fig. 1 A timeline illustrating the relationships between polysomnographic monitoring, $H_2{}^{15}O$ injection, blood sampling and PET data collection.

were instructed to remain awake for the first scan. If they appeared to be falling asleep the polysomnographer would wake them within 1–2 s, and the wakefulness scan was then repeated. Following the wakefulness study, subjects were allowed to sleep. PET scans were performed during Stage 3–4, i.e. slow wave sleep (SWS), and REM sleep. These stages were identified polysomnographically using the sleep-stage scoring procedure of Rechtschaffen and Kales (1968). For inclusion in the present analyses, each PET scan had to occur during a sleep stage that was uniformly maintained (i.e. was free of arousals and stage shifts) from 40 s before, to 40 s after the arrival of the $H_2{}^{15}O$ bolus in the brain (Fig. 1). A second waking study was performed at the end of the sleep period, following $\geqslant$15 min of continuous wakefulness. The two wakefulness scans were performed under the assumption that the first would probably reflect 'hypnogenic' processes in effect prior to sleep induction, while the second would reflect the effects of the intervening period of recovery sleep.

Not all 37 subjects provided complete sets of sleep/wakefulness data; pre-sleep wakefulness scans were obtained in 32 subjects; Stage 3–4 scans in 22 subjects; REM-sleep scans in 10 subjects and post-sleep-wakefulness scans in 22 subjects. The number of subjects included in the pairwise contrasts (i.e. the number in whom scans were obtained for each pair of sleep–wakefulness stages) were as follows: pre-sleep wakefulness–SWS, 20 subjects; SWS–post-sleep wakefulness, 14 subjects; SWS–REM sleep, seven subjects; pre-sleep wakefulness–REM sleep, eight subjects; REM sleep–post-sleep wakefulness, seven subjects; pre-sleep wakefulness–post-sleep wakefulness, 20 subjects.

Scanning methods

PET scans were performed on a Scanditronix PC2048–15B tomograph (Uppsala, Sweden) which has an axial and in-plane resolution of 6.5 mm. Fifteen planes, offset by 6.5 mm (centre to centre), were acquired simultaneously, parallel to the cantho-meatal line. When a target stage was identified polysomnographically, 30 mCi of $H_2{}^{15}O$ were injected as an intravenous bolus. Scans were initiated automatically when the radioactive count rate in the brain reached a threshold value (~20 s after intravenous injection) and continued for 4 min (Fig. 1). Sixteen scan frames were collected dynamically during this 4-min period (12 10-s scans followed by four 30-s scans). Studies were separated by intervals of $\geqslant$12 min. Emission data were corrected for attenuation by means of a transmission scan obtained at the same levels.

Arterial blood was sampled automatically throughout the scanning period, and PET scans and arterial time–activity data were used to produce rCBF images employing a rapid least squares method (Koeppe *et al*., 1985). At the completion of each scan a final arterial blood sample was collected and pCO_2 measurements were performed (Fig. 1). These measures were utilized for pCO_2 correction of measured CBF rates, as described below.

Image averaging and spatial normalization

PET scans were registered and analysed using statistical parametric mapping (SPM) software (MRC Cyclotron Unit, Hammersmith Hospital, London, UK). The 15 original PET planes of section were trilinearly interpolated to yield 43 planes in which voxels were approximately cubic. For each subject, final parametric rCBF images were registered using image-alignment software in order to minimize the effects of head movement. Images were smoothed with a Gaussian filter (20 $\times$ 20 $\times$ 12 mm in the *x*, *y* and *z* axes) in order to accommodate inter-subject differences in anatomy, and stereotaxically normalized using a nonlinear transformation to produce images of 26 planes parallel to the anterior–posterior commissural line in a common stereotaxic space (Friston *et al*., 1989) with a voxel size of 2 $\times$ 2 $\times$ 4 mm, cross-referenced with a standard anatomical atlas (Talairach and Tournoux, 1988).

Absolute and normalized rCBF values

For analysis of absolute rCBF, images were first corrected for changes in measured pCO_2 (Reiman *et al*., 1986). In several instances, PET data collection was completed during a sleep stage that was uniformly maintained, but a stage shift or intervening arousal occurred prior to collection of arterial blood for measurement of pCO_2. In these instances, pCO_2 was estimated using data which had been collected in the remaining subjects; pCO_2 values obtained during any one stage were regressed on levels obtained during a second

stage, and the derived regression equation was used to estimate values for subjects in whom pCO_2 values in the second stage were missing.

For evaluation of absolute pCO_2-corrected CBF, images were analysed without further treatment. Global flow rates were calculated for each subject by averaging grey matter pixel values for scans obtained during each stage. Between-stage differences in global CBF were evaluated separately by analysis of variance (ANOVA).

Analyses of normalized rCBF were performed in two ways. Using the first method, differences in global CBF were controlled for by analysis of covariance (ANCOVA) with measured global flow as the covariate. This permitted calculation of an adjusted-error variance associated with mean flow in each voxel (Friston *et al*., 1990). Using the second method, the global rate was used to normalize each image, generating reference ratios (regional : global CBF) on a pixel-by-pixel basis.

Stage-specific changes in rCBF were evaluated for absolute, ANCOVA-corrected and reference-ratio-normalized data sets, using the *t* statistic calculated for all voxels in parallel (Friston *et al*., 1991). The resulting set of values, transformed to *Z*-scores, constitutes a statistical parametric map (SPM{*Z*}). For these comparisons the profile of significant rCBF change was defined as the subset of voxels exceeding a threshold of 2.57 in absolute value (equivalent to $P < 0.005$).

Selected rCBF values were extracted from individual PET scans in a separate procedure, for purposes of illustration. Coordinates of representative centrencephalic, paralimbic and neocortical regions were selected using the Talaraich atlas and adjusted using the canonical PET template contained in SPM. Regional values were derived, using these coordinates, from stereotaxically normalized, reference-ratio-adjusted images, smoothed with a $20 \times 20 \times 12$ mm Gaussian filter as described above. Values for homologous regions in right and left hemispheres (obtained by reversing the sign of the *x*-coordinate in Talairach space) were averaged. Data were obtained from all subjects in whom the various sleep or wakefulness stages were acquired, and therefore were not limited by the subject numbers to which the pairwise contrasts were restricted. These data were not used for statistical comparisons, but to illustrate changes in normalized rCBF across the sleep–wake cycle.

Complementary evaluation of absolute and normalized data

Differences in absolute CBF rates, when detected, may be more meaningful than changes in normalized rates. This is particularly true in the present study, in which sleep stage contrasts were characterized by significant shifts in global flow rates, information which is obscured when data are normalized. On the other hand, significant differences are often more readily detected and regional heterogeneity is frequently more apparent when normalized values are analysed, i.e. when inter-subject differences in global flow are controlled for. In the present analysis, both absolute and normalized datasets were evaluated conjointly.

When comparing two sleep stages, absolute pCO_2-corrected global flow rates were in each instance evaluated first. If significant between-stage differences in global flow were detected, normalized blood-flow rates are reported but interpreted in context. For example, if only decreases were observed in absolute CBF rates in comparing two sleep stages, only decreases in normalized comparisons were considered as indices of real change. On the other hand, increases in normalized flow rates (in the context of absolute decreases) were interpreted as identifying brain regions in which absolute values deviated the least, i.e. regions associated with invariance or minimal, non-significant decreases in absolute rCBF. On the other hand, if significant differences in absolute pCO_2-corrected global flow were not detected, normalized comparisons are simply reported as indices of relative change.

Evaluation of hemispheral differences in rCBF

A modification of SPM software was used to evaluate hemispheral differences in the magnitude of regional activation or deactivation. Stage-related differences in normalized rCBF for each contrast were compared between homologous pixels in right and left hemispheres (defined by reversing the sign of the *x*-coordinate in Talairach space), using a voxel-wise error variance calculated for such differences in each contrast. Right–left differences exceeding a threshold of 2.57 in absolute value are reported, as indicated, in Tables 1–4.

Results

Non-REM sleep

Presleep-wakefulness to SWS

Compared with pre-sleep wakefulness, Stage 3–4 (deep sleep, SWS) was characterized by a global reduction in pCO_2-corrected CBF of 26.0% ($P < 0.001$; Fig. 2). Since only reductions were observed in the analysis of absolute flow, only reductions in normalized flow rates were considered as indices of real change; increases in normalized flow rates, on the other hand, identified brain regions in which absolute values were associated with invariance or minimal, non-significant differences (Table 1).

Among centrencephalic structures (Fig. 3; Table 1) the most significant reductions in ANCOVA-corrected rCBF during Stage 3–4 sleep were found in the posterior putamen, with significant, but less robust, reductions evident in the caudate nucleus. Significant decreases were detected throughout the midbrain (larger in the tegmentum than the periaqueductal grey), with smaller decreases in the lower pontine tegmentum. SWS was associated with significant reductions in rCBF throughout the basal forebrain (caudal

Table 1 *Slow wave sleep (SWS) versus pre-sleep wakefulness*

Regions	Brodmann area	*Z*-score	Talaraich coordinates			ΔrCBF
			x	*y*	*z*	
Centrencephalic						
Cerebellum						
Hemisphere		–4.77	–34	–78	–28	–5.33
Vermis		3.18	2	–58	–12	2.89
Brainstem						
Pons		–3.53	–4	–36	–28	–5.39
Midbrain tegmentum		–5.34	–14	–18	0	–7.72
Midbrain PAG		–4.77	–4	–24	–4	–7.45
Thalamus						
Ventral posterior		–5.56	–16	–20	4	–8.22
Pulvinar		–5.16	–14	–24	8	–8.53
Centrum medianum		–5.30	–8	–20	0	–9.76
Dorsomedial		–4.24	–6	–18	8	–11.69
Basal ganglia						
Ventral striatum		–4.15	16	6	–8	–4.60
Caudate		–4.54	12	6	8	–4.55
Putamen		–6.09	–26	–4	–4	–5.07
Basal forebrain						
AH-POA		–4.19	–2	–8	–4	–5.81
Caudal orbital		–3.44	14	18	–16	–4.00
Paralimbic–limbic						
Temporal polar						
Temporal pole	38	–2.65	44	16	–8	–2.93
Insula						
Anterior insula		–4.98	38	6	0	–6.11
Posterior insula		2.68	–40	–22	4	1.40
Cingulate						
Anterior cingulate	32	–4.08	–4	24	28	–6.32
Posterior cingulate	23	3.34	10	–58	8	3.74
Neocortical						
Prefrontal						
Medial orbital		–3.75	18	58	–4	–3.47*
Medial prefrontal	10	–4.06	16	58	12	–2.83
Lateral orbital	11	–4.37	26	48	–12	–4.38
Dorsolateral prefrontal	46	–4.47	–42	36	16	–3.52
Opercular	45	–3.88	44	22	8	–3.34
Unimodal sensory						
Superior temporal gyrus	22	3.27	–56	–22	4	2.86
Inferior temporal gyrus	37, 19	3.40	–46	–48	–4	2.68
Fusiform gyrus	37, 19	3.62	20	–58	–8	3.99
Lateral occipital	18, 19	3.52	–36	–76	12	3.70
Striate	17	4.73	10	–82	4	8.16
Heteromodal sensory						
Middle temporal–STS	21	4.73	–46	–34	0	5.19
Angular gyrus	39	–3.30	52	–42	24	–2.48
Supramarginal gyrus	40	–3.47	50	–44	28	–4.02

Regions in which ANCOVA-corrected rCBF levels differ from baseline are tabulated along with *Z*-scores (representing local maxima or minima and associated Talairach coordinates); ΔrCBF = change in rCBF (ml/100 g/min, normalized to a mean of 50). PAG = periaqueductal grey; STS = superior temporal sulcus; AH-POA = anterior hypothalamus-pre-optic area. Instances in which rCBF responses exceeded threshold in one hemisphere only and significant differences between right and left hemispheres were detected ($Z > 2.57$ in absolute value) are indicated with asterisks (*right hemisphere alone).

orbital cortex, anterior hypothalamus–preoptic area and ventral regions of the striatum). Significant decreases were also observed in the inferior cerebellar hemispheres, but not in more dorsal regions of the neocerebellum or in the cerebellar vermis, where positive *Z*-scores indicated invariance in absolute flow.

Table 2 *REM sleep versus slow wave sleep (SWS)*

Regions	Brodmann area	*Z*-score	Talaraich coordinates			ΔrCBF
			x	*y*	*z*	
Centrencephalic						
Cerebellum						
Vermis		2.57	–24	–56	–12	2.96
Brainstem						
Pons		2.61	–8	–36	–28	10.97
Midbrain tegmentum		3.09	14	–12	0	8.94
Midbrain PAG		2.61	–10	–28	–4	10.88
Thalamus						
Ventral lateral		3.02	14	–12	4	8.56
Centrum medianum		2.59	8	–16	0	10.24
Pulvinar		3.32	–14	–24	8	8.01
Anterior		2.82	12	–4	8	6.68
Basal ganglia						
Ventral striatum		2.82	–6	16	–8	5.49
Caudate		7.98	–8	8	12	6.06
Putamen		3.63	22	–12	0	5.75
Basal forebrain						
AH-POA		2.87	4	–6	–8	9.18
Caudal orbital		7.98	–2	20	–4	5.61
Paralimbic–limbic						
Mesial temporal						
Parahippocampal gyrus	37	3.37	–26	–48	–8	4.94
Hippocampus		3.13	–24	–34	–4	4.33
Temporal pole						
Temporal polar	38	2.79	42	4	–8	2.83
Insula						
Anterior insula		2.97	36	2	–4	4.09
Posterior insula		–2.74	–38	–24	0	–5.41
Cingulate						
Anterior cingulate	32	3.42	–6	40	8	5.30
Posterior cingulate	23	–4.52	–8	–36	28	–2.60
Neocortical						
Prefrontal						
Medial prefrontal	10	2.97	6	56	16	4.47
Lateral orbital	11	–3.36	–26	52	–4	–2.79
Dorsolateral prefrontal	46	–2.80	–38	34	12	–3.26
Opercular	45	–3.47	–46	26	0	–3.09*
Unimodal sensory						
Superior temporal gyrus	22	2.57	46	0	–4	4.47
Inferior temporal gyrus	37, 19	3.17	–38	–58	–12	2.11
Fusiform gyrus	37, 19	3.22	–30	–54	–8	3.29*
Heteromodal sensory						
Middle temporal–STS	21	–2.90	–44	–46	0	–3.38
Angular gyrus	39	–4.52	28	–74	24	–3.00

Regions in which ANCOVA-corrected rCBF levels differ from baseline are tabulated along with *Z*-scores (representing local maxima or minima and associated Talairach coordinates; ΔrCBF = change in rCBF (ml/100 g/min, normalized to a mean of 50). In no instances were significant differences between right and left hemispheres detected. PAG = periaqueductal grey; STS = superior temporal sulcus; AH-POA = anterior hypothalamus-pre-optic area. Instances in which rCBF responses exceeded threshold in one hemisphere only and in which significant differences between right and left hemispheres were detected ($Z > 2.57$ in absolute value) are indicated with an asterisk (*left hemisphere alone).

SWS was also characterized by reduced CBF throughout the thalamus. The most statistically robust decreases were found in the sensory relay nuclei and the centrum medianum, while less robust changes in rCBF (ΔrCBF) were observed in regions of the thalamus related to prefrontal (dorsomedial nucleus) motor cortex (ventrolateral nucleus, *Z*-score = –4.28; ΔrCBF = –8.66 ml/100 g/min; Talairach $x = -12$, $y = -14$, $z = 8$) or limbic cortices (anterior nucleus, –3.48;

Table 3 *REM versus pre-sleep wakefulness, post-sleep wakefulness and slow wave sleep (SWS)*

Regions of interest	Brodmann area	REM versus SWS					REM versus pre-sleep wakefulness					REM versus post-sleep wakefulness				
		Z-score	*x*	*y*	*z*	ΔrCBF	*Z*-score	*x*	*y*	*z*	ΔrCBF	*Z*-score	*x*	*y*	*z*	ΔrCBF
REM > SWS, wakefulness																
Centrencephalic																
Cerebellar vermis		2.57	–24	–56	–12	2.96	2.95	18	–46	–12	4.98	2.90	–12	–56	–8	3.27
Pons		2.61	–8	–36	–28	10.97	3.28	–2	–18	–24	8.50	4.92	8	–16	–20	4.42**
Midbrain		3.07	14	–12	0	8.94	2.63	–14	–28	–16	5.27	4.92	8	–12	–16	3.72
Caudate		7.98	–8	8	12	6.06	3.03	–4	18	8	3.94	3.35	–6	14	12	1.52
Caudal orbital		7.98	–2	20	–4	5.61	2.67	–2	18	–20	4.31	–	–	–	–	–
Paralimbic–limbic																
Parahippocampal gyrus	37	3.37	–26	–48	–8	4.94	3.06	–16	–26	–20	4.90	3.20	–18	–50	–8	4.33
Hippocampus		3.13	–24	–34	–4	4.33	3.71	24	–40	–8	2.39	3.30	22	–18	–12	2.25
Anterior cingulate	32	3.42	–6	40	8	5.30	2.74	4	30	0	3.39	2.90	2	34	4	2.42
Neocortical																
Medial prefrontal	10	2.97	6	56	16	4.47	2.82	–2	44	24	1.79	–	–	–	–	–
Inferior temporal gyrus	37, 19	3.17	–38	–58	–12	2.11	–	–	–	–	–	3.30	28	–66	4	2.62
Fusiform gyrus	37, 19	3.22	–30	–54	–8	3.29*	3.03	24	–40	–12	3.42	3.40	22	–58	–4	3.86
SWS, wakefulness > REM																
Paralimbic–limbic																
Posterior insula		–2.74	–38	–24	0	–5.41	–4.47	28	–30	20	–1.75	–2.49	28	–42	20	–1.21
Posterior cingulate	23	–4.52	–8	–36	28	–2.60	–2.57	–6	–32	28	–4.50	–7.98	–12	–32	24	–3.28
Neocortical																
Lateral orbital	11	–3.36	–26	52	–4	–2.79	–3.28	–30	38	–12	–4.99	–3.93	18	48	–16	–3.02
Dorsolateral prefrontal	46	–2.80	–38	34	12	–3.26	–3.97	44	32	20	–2.52	–7.98	32	44	20	–2.78
Opercular	45	–4.07	–46	26	0	–3.09*	–3.14	46	18	8	–2.93	–7.98	38	34	–12	–4.82
Angular gyrus	39	–4.52	28	–74	24	–3.00	–2.70	54	–54	24	–4.11	–7.98	30	–50	24	–1.51
Supramarginal gyrus	40	–	–	–	–	–	–2.60	46	–42	24	–5.68	–7.98	–38	–46	28	–4.06

Regions in which ANCOVA-corrected rCBF levels differ from baseline with *Z*-scores at local maxima or minima; ΔrCBF = change in rCBF (ml/100 g/min, normalized to a mean of 50). Instances in which rCBF responses exceeded threshold in one hemisphere only and significant differences between right and left hemispheres were detected ($Z > 2.57$ in absolute value), are indicated with asterisks (*left hemisphere alone, **right hemisphere alone).

Table 4 *Post- versus pre-sleep wakefulness*

Regions	Brodmann area	*Z*-score	Talaraich coordinates			ΔrCBF
			x	*y*	*z*	
Hippocampus		–3.51	–34	–30	–8	–2.00
Dorsolateral prefrontal	9	–2.58	30	34	32	–1.58
Superior temporal gyrus	22	–2.97	58	–34	8	–1.52
Inferior temporal gyrus	37, 19	–3.49	56	–50	–4	–2.00
Lateral occipital	18, 19	–2.70	40	–76	12	–2.74
Striate cortex	17	–2.75	–12	–98	–8	–3.51
Middle temporal–STS	21	–3.10	56	–46	0	–2.00
Angular gyrus	39	–2.57	–48	–64	24	–2.36
Cerebellum		2.64	–2	–46	–4	2.20
Pons		2.72	10	–42	–28	3.95
Caudate		3.09	–10	–6	20	4.42
AH-POA		2.79	–8	4	–12	3.07

Regions in which ANCOVA-corrected rCBF levels differ from baseline are tabulated along with *Z*-scores (representing local maxima or minima and associated Talairach coordinates). Negative *Z*-scores indicate instances in which values during post sleep wakefulness are less than those during pre-sleep wakefulness. ΔrCBF = change in rCBF (ml/100 g/min, normalized to a mean of 50). In no instances were significant differences between right and left hemispheres detected. STS = superior temporal sulcus; AH-POA = anterior hypothalamus pre-optic area.

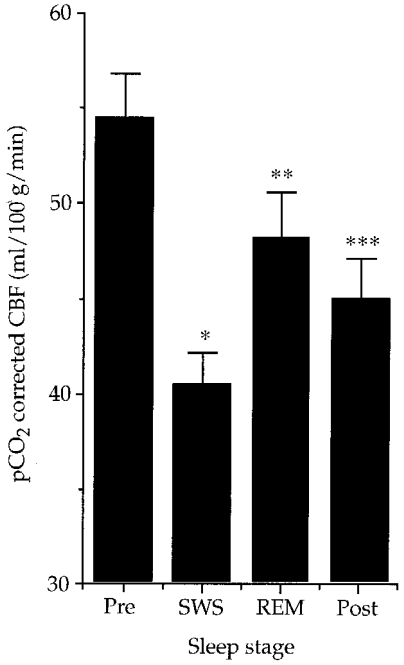

Fig. 2 Bar graph illustrating global CBF during stages of sleep and wakefulness. Bars represent absolute pCO_2-corrected CBF rates (ml/100 g/min, mean ± SEM). *$P < 0.001$ versus pre-sleep wakefulness, $P < 0.04$ versus REM sleep, $P < 0.02$ versus post-sleep wakefulness; **not significant versus pre-sleep and post-sleep wakefulness, $P < 0.04$ versus SWS; ***$P < 0.002$ versus pre-sleep wakefulness, $P < 0.02$ versus SWS, not significant versus REM sleep. The pCO_2 values for each stage were as follows: pre-sleep wakefulness, 41.6 ± 0.9 mmHg (mean ± SEM); SWS, 45.5 ± 0.7; REM sleep, 40.3 ± 2.8; post-sleep wakefulness, 40.8 ± 0.9.

–5.61 ml/100 g/min; –12, –6, 12). While decreases of the greatest magnitude were observed in the dorsomedial thalamus, constituting the largest reductions in both ANCOVA-corrected and absolute flow rates (ΔrCBF = –24.55 ml/100 g/min, $x = –2$, $y = –20$, $z = 8$), the inter-subject variance in this region was relatively high. When a subtractive approach is used, such as that applied in the present study, the centre of an activated area can often be located with relative precision despite the limited spatial resolution of the PET technique (Fox *et al*., 1986). However, it should be made clear that the peaks of activity in individual thalamic nuclei reported here represent local maxima (or minima) and not explicit anatomical structures.

SWS was associated with significant deactivation of paralimbic regions of the brain (Fig. 3; Table 1) including the anterior cingulate cortex, the anteroinferior portions of the insula and related regions of the temporal pole. Decreases in ANCOVA-corrected rCBF in mesial temporal structures including the hippocampus, parahippocampal gyrus and amygdala did not reach statistical significance. In both the posterior insula and posterior cingulate cortices, on the other hand, positive *Z*-scores indicated invariance in absolute CBF rates.

In the neocortex, changes in rCBF were heterogeneous (Fig. 3; Table 1). Significant decreases were detected only in higher order, heteromodal association cortices. These were evident throughout the prefrontal association areas including the frontal operculum, lateral orbital and dorsolateral prefrontal cortices, and were greatest in the orbital and inferior prefrontal regions. Changes in the medial orbital and medial prefrontal cortices were smaller and were detected in the right hemisphere only. In parallel with deactivation of the frontal association cortices, rCBF rates in heteromodal sensory association areas of the inferior parietal lobule, in

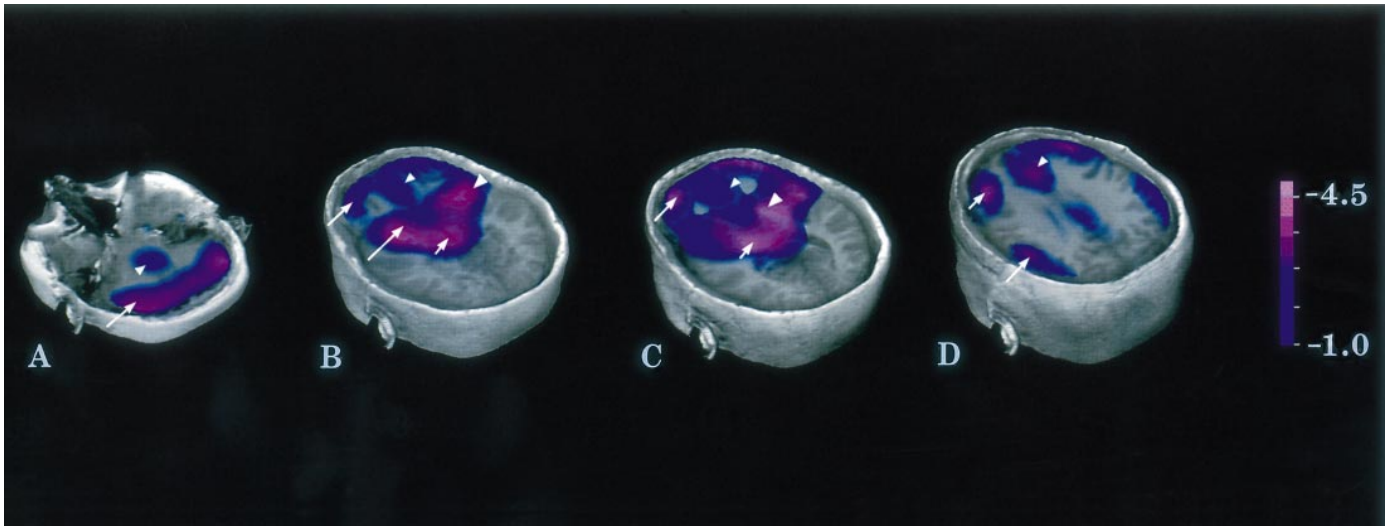

Fig. 3 Brain map illustrating decreases in rCBF during slow wave sleep (SWS), when compared with pre-sleep wakefulness as baseline. The statistical parametric (SPM{*Z*}) map illustrating changes in rCBF is displayed on a standardized MRI scan. The MRI data were transformed linearly into the same stereotaxic (Talairach) space as the SPM{*Z*} data. Using Voxel View Ultra (Vital Images, Fairfield, Ia., USA), SPM and MRI data were volume-rendered into a single three-dimensional image. The volume sets are truncated and displayed at selected planes of interest. Planes of section are located at –27 mm (**A**), 0 mm (**B**), +13 mm (**C**) and +27 mm (**D**) relative to the anterior commissural–posterior commissural line. Values are *Z*-scores representing the significance level of changes in normalized rCBF in each voxel; the range of scores is coded in the accompanying colour table, with light purple designating significant negative *Z*-scores of –4.5 and below. Significant decreases in rCBF during SWS were observed in centrencephalic structures including pons (**A**, arrowhead), midbrain (**B**, short arrow), basal ganglia (**B**, long arrow; **C**, medium arrowhead), thalamus (**C**, short arrow), caudal orbital cortex–basal forebrain (**B**, small arrowhead) and cerebellum (**A**, arrow). Similar decreases were also found in paralimbic regions of interest including anterior insula (**B**, medium arrowhead) and anterior cingluate cortices (**C** and **D**, small arrowheads). SWS was associated with significant reductions in rCBF in heteromodal association cortices of the orbital (**B**, medium arrow), dorsolateral prefrontal (**C**, medium arrow; **D**, small arrow) and inferior parietal lobes (**D**, medium arrow), but not in unimodal (visual or auditory) occipitotemporal sensory cortices (*see* Table 1).

the angular and supramarginal gyri, were also significantly reduced during SWS.

On the other hand, unimodal sensory areas of the temporal and occipital lobes (including primary and secondary visual and auditory association cortices in the superior temporal gyri, striate cortex, fusiform, lateral occipital and inferior temporal gyri) were associated with *Z*-scores which indicated invariance in absolute flow rates (Table 1). Relatively small decreases in the peri-rolandic areas (the primary motor cortex and unimodal somatosensory regions of the parietal cortex) did not reach statistical significance. In contrast to the frontal and parietal association cortices, activity in heteromodal temporal regions (Brodmann areas 20 and 21 in middle temporal gyrus and superior temporal sulcus) did not decrease.

SWS versus post-sleep wakefulness

When post-sleep wakefulness studies were compared with SWS, the significant changes mirrored those outlined above; compared with SWS, post-sleep wakefulness was characterized by a global increase in pCO_2-corrected CBF of 11.4% ($P < 0.02$; Fig. 2). The most robust elevations in normalized rCBF in post-sleep wakefulness were observed in the putamen (*Z*-score = 7.98; ΔrCBF = 7.90 ml/100 g/min; Talairach $x = -18$, $y = 0$, $z = 4$), pons (7.98; 8.37; –2, –42, –24), basal forebrain (7.98; 7.52; 4, 2, 4), thalamus (7.98; 9.04; 14, –10, 8), midbrain (4.83; 8.93; 8, –16, –4), cerebellar hemispheres (4.31; 8.4; –32, –74, –28), anterior cingulate (4.27; 5.7; 2, 36, 4), lateral orbital (4.32; 4.48; 18, 46, –12) and dorsolateral prefrontal cortices (3.38; 3.35; 36, 52, 4). Mirroring the changes observed in the pre-sleep wakefulness–SWS contrast, the greatest elevations in absolute CBF rates when SWS was compared with post-sleep wakefulness, were found in the dorsomedial thalamus (ΔrCBF = +19.05 ml/100 g/min, $x = 4$, $y = -16$, $z = 8$).

At the same time, sensory areas of the temporal and occipital lobes were associated with negative *Z*-scores, in this case indicating minimal differences in absolute flow rates between SWS and post-sleep wakefulness studies: lateral occipital cortex (*Z*-score = –5.89; ΔrCBF = –4.5 ml/100 g/min; Talairach $x = -32$, $y = -75$, $z = 12$), striate cortex (–4.53; –7.88; 16, –84, 4), inferior temporal (–3.95; –2.51; 44, –62, –4), middle temporal (–3.53; –2.66; –38, –58, 0) and superior temporal gyri (–3.25; –4.7; –52, –24, 0).

REM sleep

SWS to REM sleep

The transition from SWS to REM sleep was characterized by a global increase in pCO_2-corrected CBF of +16.8% ($P < 0.04$; Fig. 2). Since only increases were observed in

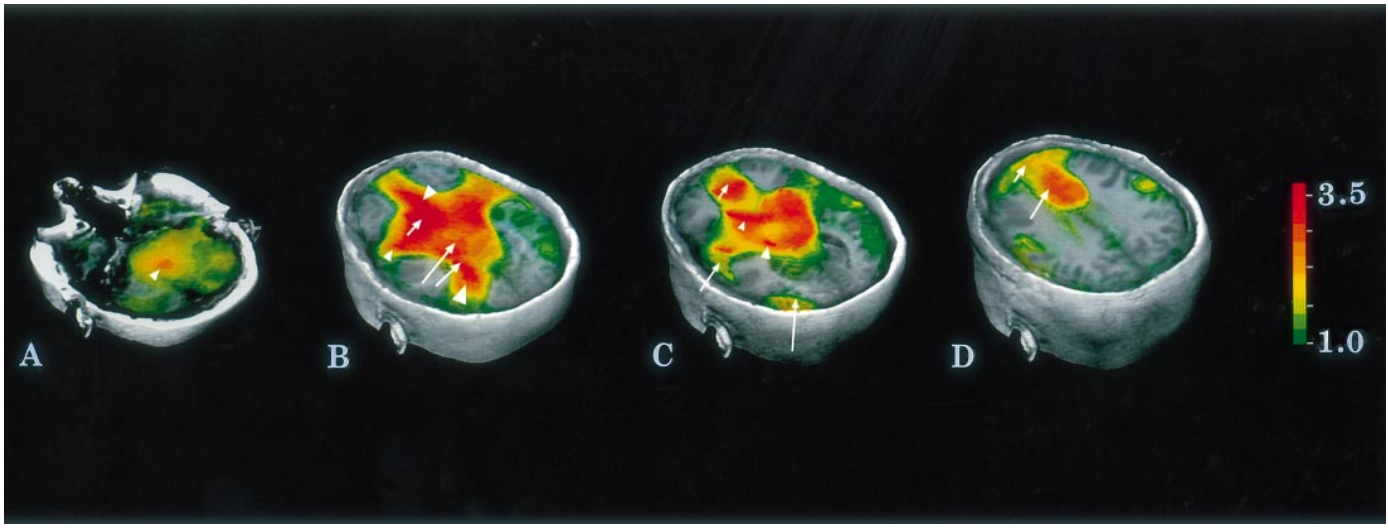

Fig. 4 Brain map illustrating increases in rCBF during REM sleep when compared with slow wave as baseline, prepared using methods outlined in the legend to Fig. 3. Values are *Z*-scores representing the significance level of changes in normalized rCBF in each voxel; the range of scores is coded in the accompanying colour table, with red designating *Z*-scores of 3.5 and above. Planes of section are located at –25 mm (**A**), +1 mm (**B**), +8 mm (**C**) and +27 mm (**D**) relative to the anterior commissural–posterior commissural line. Significant increases in rCBF during REM sleep were observed in centrencephalic structures including pons (**A**, arrowhead), midbrain (**B**, long arrow), basal ganglia (**B**, short arrow; **C**, small arrowhead), thalamus (**C**, medium arrowhead) and caudal orbital cortex–basal forebrain (**B**, medium arrowhead). Increases were also found in paralimbic regions including the anterior insula (**B**, small arrowhead), anterior cingluate (**C**, small arrow; **D**, medium arrow) and mesial temporal (parahippocampal) cortices (**B**, medium arrow). REM sleep was associated with significant elevations in rCBF in unimodal sensory cortices including inferior visual association [fusiform–inferotemporal (**B**, large arrowhead) and lateral occipital (**C**, long arrow)] and auditory association cortices (**C**, medium arrow), as well as the medial prefrontal cortex (**D**, small arrow). On the other hand, activity in heteromodal association cortices of the orbital, dorsolateral prefrontal and inferior parietal lobes, did not differ from levels observed during SWS (*see* Table 2).

the analysis of absolute flow, only increases in normalized flow rates were considered as indices of real change; decreases in normalized flow rates from SWS to REM sleep, on the other hand, identified brain regions in which absolute values were associated with invariance or minimal, non-significant change in the transition from SWS to REM sleep (Table 2).

Among centrencephalic structures (Fig. 4; Table 2), the most significant increases in rCBF were again seen in the basal ganglia, greater in the caudate nuclei than the putamen. Significant increases were also observed in the basal forebrain (anterior hypothalamus, caudal orbital cortex and ventral regions of the striatum), and in the midline anterior cerebellum and vermis. Significant increases were evident in all regions of the brainstem. The greatest increase in both ANCOVA-corrected and absolute flow rates (ΔrCBF = +15.72 ml/100 g/min, $x = -4$, $y = -40$, $z = -28$), was found in the pontine tegmentum.

In the thalamus, increases in rCBF were greatest in the sensorimotor nuclei, limbic-related nuclei of anterior thalamus and centrum medianum. While activity in the dorsomedial nucleus increased as well, inter-subject variability in this region was relatively high (as was the case in the transition from wakefulness to SWS), and the associated *Z*-score (2.40; ΔrCBF = 10.11 ml/100 g/min; Talairach $x = 4$, $y = -10$, $z = 4$) was of borderline significance.

Compared with SWS, REM sleep was characterized by activation of paralimbic and limbic areas, including the hippocampal formation and parahippocampal gyri, the anteroinferior portions of the insula and the anterior cingulate cortices (Fig. 4; Table 2). The posterior insular and posterior cingulate cortices, on the other hand, were associated with negative *Z*-scores, indicating invariance in absolute blood-flow rates.

In the neocortex, changes in rCBF were again heterogeneous (Fig. 4; Table 2). In the frontal cortex, significant increases in CBF during REM sleep were detected only in the medial prefrontal cortices. In the remaining frontal association areas (i.e. lateral orbital, dorsolateral prefrontal and opercular cortices, areas in which CBF had been attenuated in the transition from wakefulness to SWS) activity remained attenuated during REM sleep; i.e. these regions were associated with negative *Z*-scores which indicated invariance in absolute flow rates.

Similarly, activity in the heteromodal association cortices of the inferior parietal lobule, which decreased significantly in the transition to SWS, did not differ during REM sleep from the levels which were observed during SWS. In heteromodal regions of the temporal lobe, Brodmann areas 20 and 21 in middle temporal gyrus and superior temporal sulcus, negative *Z*-scores indicated statistical invariance, i.e. absolute values did not differ from levels observed during SWS (Table 2).

On the other hand, significant increases in rCBF during REM sleep were observed in post-rolandic unimodal sensory cortices (Fig. 4; Table 2) including visual association areas

(mesial and inferior temporal cortices) and auditory association cortices of the superior temporal gyrus.

REM sleep versus wakefulness studies

Although there was a trend toward higher global CBF rates during REM sleep than post-sleep wakefulness, and lower rates during REM sleep than pre-sleep wakefulness studies, absolute rCBF values in REM sleep did not differ significantly from those measured during either period of wakefulness (Fig. 2). In the absence of significant differences in absolute flow, significant increases and decreases in ANCOVA-corrected rCBF values are interpreted as indices of *relative* change.

When REM sleep-activity is compared with activity in each of the other states separately (Table 3), the associated spatial distributions are remarkably congruent; rCBF rates in regions which were activated during REM sleep (compared with non-REM sleep) were also relatively higher in REM sleep than in either pre-sleep or post-sleep wakefulness studies. That is, regional cerebral activity during REM sleep was not only elevated above the relatively low levels observed during SWS, but above wakefulness levels as well.

Compared with pre-sleep wakefulness studies, the largest elevations in normalized rCBF during REM sleep were found in the pontine tegmentum. Other centrencephalic areas in which normalized activity during REM sleep exceeded wakefulness levels included the midbrain, the basal forebrain–caudal orbital regions, caudate nucleus, and cerebellar vermis. However, unlike the SWS–REM sleep comparison, normalized rCBF in the thalamus did not differ significantly from levels measured during wakefulness.

In paralimbic regions, activity during REM sleep exceeded pre-sleep wakefulness levels in the hippocampus and parahippocampal cortices, and in the anterior but not posterior cingulate cortex. Normalized rCBF rates in the posterior insula were significantly lower during REM sleep than during pre-sleep wakefulness. While activity in the anterior insula was higher during REM sleep than SWS, elevations in anterior insular activity when REM sleep was compared with pre-sleep wakefulness did not reach statistical significance.

In the frontal lobe, normalized activity in the medial prefrontal cortex was significantly higher during REM sleep, while activity in the lateral orbital, dorsolateral prefrontal and frontal opercular cortices was significantly lower during REM sleep than pre-sleep wakefulness. Activity in the heteromodal association cortices of the inferior parietal lobule was similarly reduced during REM sleep. On the other hand, as was the case in the SWS–REM sleep contrast, normalized rCBF was significantly higher during REM sleep than during pre-sleep wakefulness in post-rolandic unimodal sensory areas including the visual association areas of the fusiform and lateral occipital gyri.

When REM sleep and post-sleep wakefulness studies were compared, a similar pattern was evident (Table 3). There were robust elevations of normalized rCBF, during REM sleep, in the pons, midbrain, caudate nucleus, cerebellar vermis, hippocampus and parahippocampal gyrus, anterior cingulate, and fusiform and inferior temporal gyri. Activity was significantly lower during REM sleep than during post-sleep wakefulness in prefrontal association (dorsolateral, orbital and opercular) and inferior parietal (angular and supramarginal) association cortices, as well as posterior insular and posterior cingulate cortices. Figure 5 illustrates relative increases in rCBF in the latter regions when post-sleep wakefulness studies are contrasted with REM sleep as baseline, i.e. the relative increases which were observed in these areas during the transition from REM sleep to wakefulness. Differences between the 'REM sleep–post-sleep wakefulness' and 'REM sleep–pre-sleep wakefulness' comparisons, e.g. in basal forebrain–caudal orbital regions, may reflect differences between pre- and post-sleep studies themselves (*see* below).

Sleep deprivation, post-recovery wakefulness studies

Pre- versus post-sleep wakefulness

Global pCO_2-corrected CBF rates were significantly lower during post-sleep than during pre-sleep wakefulness studies, showing a relative decrease of 17.5% ($P < 0.002$; Fig. 2). These differences may represent either increases in CBF due to sleep deprivation or decreases brought about by intervening recovery sleep (or both).

Since only decreases during post-sleep wakefulness, compared with pre-sleep wakefulness, were observed in the analysis of absolute flow, only decreases in normalized flow rates were considered as indices of real change (Table 4). These were found, for the most part, in the neocortex, and decreases were greatest in unimodal areas of the occipital and temporal lobes, and in visual (striate, occipital, and inferotemporal association) cortices. Decreases were also observed in the superior temporal auditory association cortices. rCBF in the hippocampus was also significantly lower following recovery sleep, constituting the most statistically robust difference in the comparison of the two periods of wakefulness.

Similar, but less robust, decreases were observed in heteromodal association regions of the neocortex; in the frontal opercular, orbital and dorsolateral prefrontal regions, middle temporal gyrus–superior temporal sulcus, and the inferior parietal lobule, activity was elevated during pre-sleep wakefulness and reduced following recovery sleep (Table 4).

In contrast, centrencephalic structures, including brainstem, basal ganglia, basal forebrain and cerebellum, were associated with positive *Z*-scores, indicating invariance in absolute blood-flow rates (Table 4).

To determine whether differences in pre-scan sleep deprivation schedules impacted on CBF values measured during specific sleep stages, data from groups of subjects who underwent an average of 39 h of continuous wakefulness

(n = 6) were contrasted with data from subjects who had been allowed a 2-h non-REM sleep nap 20 h prior to the scans (n = 13). There were no differences between the groups when either global or regional CBF values were evaluated for pre- or post-sleep wakefulness studies, or SWS. (REM sleep scans were acquired only in the latter group, thus similar comparisons could not be made for this sleep stage).

Comparison of ANCOVA-corrected and reference-ratio-normalized tests of significance

Previous studies (e.g. Ramsay *et al*., 1993) suggest that induced changes in global CBF affect task- or state-dependent changes in regional CBF in an 'additive' fashion, making ANCOVA correction an appropriate method of normalization. However, in view of the large scale shifts in global CBF which we observed, we decided to determine whether or not our results would be affected by the choice of normalization procedure, by comparing ANCOVA-corrected (additive) and reference-ratio-normalized (proportional) values derived from the same data set.

The pre-sleep wakefulness to SWS transition, which resulted in the largest shift in global CBF, was selected for the complementary analysis; in this case, average global CBF values (derived for each subject during each stage) were used to normalize rCBF values. Reference ratios (local value : global mean) were calculated for each pixel in the image as outlined above, and SPM between-stage contrasts were performed using these images. Results of the ANCOVA-corrected and reference-ratio analyses were then compared. The estimated smoothness of the derived SPMs were essentially the same: 10.68 FWHM (full width half maximum) for the reference ratio, and 10.10 mm FWHM for the ANCOVA-corrected contrast (the effective FWHM for all ANCOVA-corrected contrasts reported here were between 10 and 12 mm). Maximum and minimum Z-scores calculated in both reference-ratio- and ANCOVA-corrected analyses were within the same range (+5.17, –6.09 for ANCOVA and +5.74, –5.42 for reference-ratio normalizations), and the regional distribution of these Z-scores were congruent. We may therefore conclude that our results are independent of the method used to correct for global CBF changes.

Left–right differences in rCBF

Significant lateralization of state-related rCBF changes was rarely encountered (Tables 1–4, indicated by asterisks). In a limited number of instances, differences between sleep and wakefulness stages were detected in only one hemisphere, accompanied by significant differences between hemispheres when these were tested directly. The most robust lateralized effect (z = 2.75) was seen in the pre-sleep wakefulness–SWS contrast in which significant decreases in medial prefrontal cortex were detected in the right hemisphere alone. Other than for scattered asymmetric hemisphere responses, e.g. in the frontal operculum and fusiform gyrus in the SWS–REM sleep contrast and in the pons in the REM sleep–post-sleep wakefulness contrast, such lateralized differences in rCBF were not commonly observed.

Discussion

The state-dependent changes in CBF which we observed indicate that fundamental differences in the functional organization of the brain characterize, and underlie the transitions between, wakefulness, non-REM sleep and REM sleep. Our results are in a number of instances consistent with those of previous studies (Madsen *et al*., 1991*a*, *b*) but there are also differences, due to variations in methodology and design, which suggest a complex and perhaps more comprehensive picture of brain function throughout the sleep–wake cycle.

Global changes in CBF

CBF levels, corrected for changes in arterial pCO_2, are presumed to reflect energy consumed in cerebral synapses, over and above levels required to support basal neuronal and glial metabolism (Jueptner and Weiller, 1995). Therefore, the global or overall changes we observed suggest that there is a generalized decrease in synaptic activity in the transition from wakefulness to non-REM sleep, a restoration of synaptic function during REM sleep and a secondary generalized decrease in synaptic function upon waking (following recovery sleep).

The earliest studies of CBF and metabolism during sleep were difficult to interpret, due to extant technical and methodological limitations. For example, in some instances increases in CBF during both non-REM and REM sleep were reported (Mangold *et al*., 1955; Reivich *et al*., 1968; for review *see* Franzini, 1992). However, it is now reasonably well established that SWS is associated with a decrease in global CBF, and REM sleep with values which are similar to those observed during wakefulness (Madsen and Vorstrup, 1991; Madsen *et al*., 1991*b*; Madsen, 1993; Franzini, 1992). The present results are consistent with these more recent findings (Fig. 2). In addition, the stage-specific changes in pCO_2 which we recorded (Fig. 2, legend) are consistent with changes previously reported (Robin *et al*., 1958; Douglas *et al*., 1982).

The evaluation of global flow rates also produced a somewhat paradoxical finding; when pre- and post-sleep wakefulness studies were compared, even brief periods of recovery sleep appeared to be associated with a decrease in global CBF when subjects awoke. This is consistent with at least one report in which rapid decreases in CBF velocity were detected following electroencephalographic arousal, using ultrasound techniques (Hajak *et al*., 1994).

However, the importance of global changes in CBF which take place throughout the sleep–wake cycle is not entirely clear. Since sleep-stage-related changes in blood flow,

and thus in synaptic function, appear to be regionally heterogeneous, it is probably most meaningful to identify the areas in which these differences are manifest, and to make an effort to characterize the regional patterns associated with these state-dependent changes in cerebral activity.

Regional changes in CBF

Functional significance of rCBF activation patterns

As a means of summarizing and ultimately modelling state-dependent differences in cerebral activity, the brain regions involved can be parsed into functional categories: (i) centrencephalic and subtentorial structures include the cerebellum, brainstem, basal ganglia, thalamus and the basal forebrain (which encompasses the substantia inominata, ventral regions of the striatum, anterior hypothalamus–preoptic area and caudal orbital surface of frontal lobe); (ii) paralimbic, limbic and other proiso-cortical regions include mesial temporal (amygdala, hippocampus and parahippocampal gyri), insular and cingulate cortices; (iii) neocortical regions include higher order (heteromodal) association cortices, peri-rolandic and primary and secondary post-rolandic sensory cortices. Evaluation of hemispheral differences suggest that these regional, state-dependent changes are for the most part bilateral, therefore this discussion will not focus on lateralized effects.

Centrencephalic structures

Significant changes were systematically detected throughout centrencephalic regions in all sleep–wake stage contrasts, except for the comparison of pre- and post-sleep wakefulness studies. (Tables 1–3; Figs 3 and 4). This is not surprising, since centrencephalic regions are purported to represent core elements of the major ascending systems which regulate arousal or the level of consciousness.

The work of Bremer (1935) and Mourozzi and Magoun (1949) led to the idea that the rostral brainstem's isodendritic core, i.e. the ponto-mesencephalic reticular formation (Mesulam *et al*., 1983*b*; Mitani *et al*., 1988), represents the base of an ascending reticular activating system which controls the excitability of the forebrain, and thus regulates the state of consciousness. This concept has been supported by recent investigations using contemporary techniques (Munk *et al*., 1996; Steriade, 1996).

There appear to be two major routes by which the brainstem reticular formation exerts its effects upon the cortex (Fig. 6) (Scheibel and Scheibel, 1967; Robertson *et al*., 1973; Fuller, 1975). A dorsal branch projects to the intralaminar thalamus, a direct diencephalic extension of the reticular core (Jasper, 1949; Brodal, 1981) that is situated so as to regulate cortical activity (i) through direct neocortical projections, (ii) through its associations with other thalamic nuclei or (iii) via its substantial projections to the basal ganglia.

A ventral branch of the ascending reticular activating system continues into the basal forebrain, and constitutes an alternate route by which reticular afferents may regulate cortical activity (Kanai and Szerb, 1965). The basal forebrain is the origin of widespread cholinergic projections to neocortex and paralimbic regions of the brain, which appear to play a role in cortical EEG desynchronization, and thus arousal (Semba, 1991).

In the present study, the elements of both dorsal and ventral ascending systems were deactivated during SWS (compared with wakefulness; Table 1), and this may account for the relatively increased arousal threshold that characterizes these deepest stages of non-REM sleep.

In contrast, significant increases in rCBF were evident during REM sleep (compared with SWS) in elements of both ascending systems (Table 2), consistent with the notion of a generalized activation of arousal systems during this stage. However, when REM sleep was compared with either pre- or post-sleep wakefulness studies (Table 3), activity in brainstem and basal forebrain was, in each instance, significantly elevated above wakefulness levels, while activity in the thalamus was not. This suggests that preferential activation of the ventral, or cholinergic, portion of the reticular outflow pathway may be a distinguishing feature of REM sleep.

Certain changes in the activity of centrencephalic structures appeared to be specific for REM sleep and may be related to events uniquely associated with this sleep stage (Callaway *et al*., 1987). For example, activity in both the pons and mesencephalon decreased during SWS (compared with wakefulness; Table 1) and increased during REM sleep (compared with SWS; Table 2); however, increases in the pontine tegmentum during REM were greater than those in the mesencephalon when compared with SWS or either period of wakefulness (Table 3). This is consistent with the hypothesis that cholinergic neurons of the rostral pons are specifically activated during this stage (Mitani *et al*., 1988). It has been shown, for example, that these neurons increase their activity five- to tenfold during the generation of PGO waves (McCarley and Hobson, 1971).

Similarly, activity in the cerebellar hemispheres was significantly depressed in the transition from wakefulness to SWS (Table 1), consistent with the reduction of sensorimotor function that characterizes this stage (Williams *et al*., 1964). However, during REM sleep, while blood flow in the cerebellar hemispheres remained relatively low, activity in the vermis increased significantly; normalized flow values in this region were elevated above levels observed during both SWS and wakefulness (Table 3). A selective increase in activity of the vermis during REM sleep is not unexpected since it represents the principal cerebellar target of the vestibular system, which is thought to play a cardinal role in both the generation of the rapid eye movements and presynaptic inhibition of segmental motor neurons during REM sleep (Pompeiano, 1967; Velluti *et al*., 1985).

It should be mentioned that a number of rCBF increases observed in centrencephalic structures during the transition

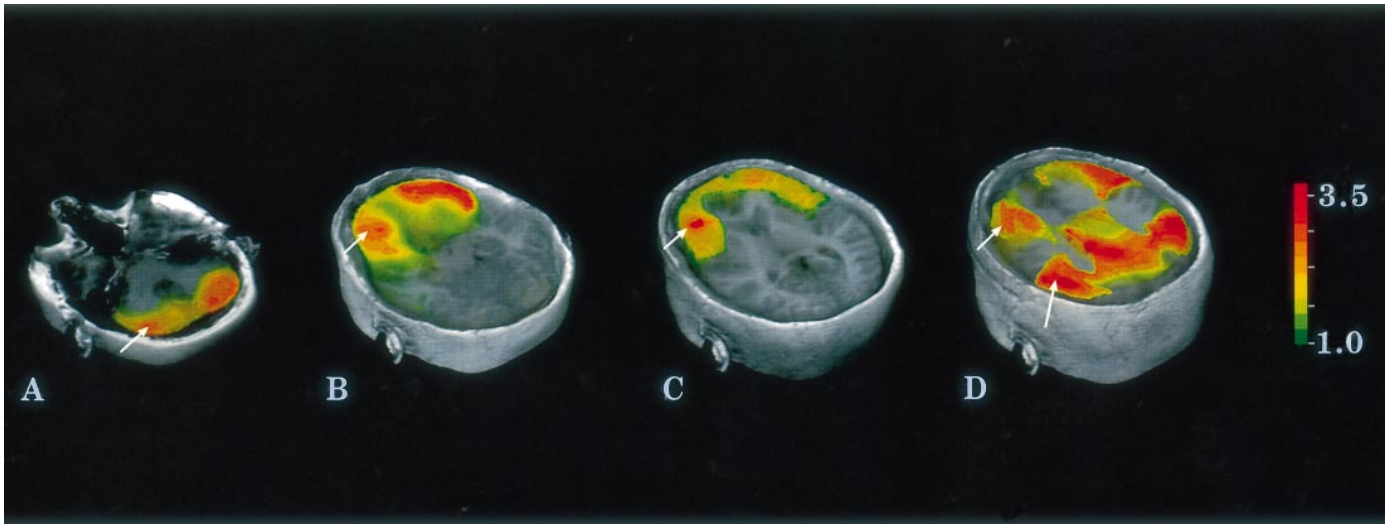

Fig. 5 Brain map illustrating increases in rCBF during post-sleep wakefulness when compared with REM sleep as baseline, prepared using methods outlined in the legend to Fig. 3. Values are *Z*-scores representing the significance level of changes in normalized rCBF in each voxel; the range of scores is coded in the accompanying colour table, with red designating *Z*-scores of 3.5 and above. Planes of section are located at –25 mm (**A**), –5 mm (**B**), +9 mm (**C**) and +27 mm (**D**) relative to the anterior commissural–posterior commissural line. The rCBF in heteromodal association cortices of the orbital (**B**, small arrow), dorsolateral prefrontal (**C** and **D**, small arrows), and inferior parietal lobes (**D**, medium arrow), which had decreased at the onset of SWS and remained depressed during REM sleep, increased significantly during the transition from REM sleep to post-sleep wakefulness. Similar increases were seen in the cerebellar hemispheres (**A**, small arrow). Activity in centrencephalic, paralimbic and post-rolandic sensory association cortices, on the other hand, was relatively higher during REM sleep than during post-sleep wakefulness (*see* Table 3).

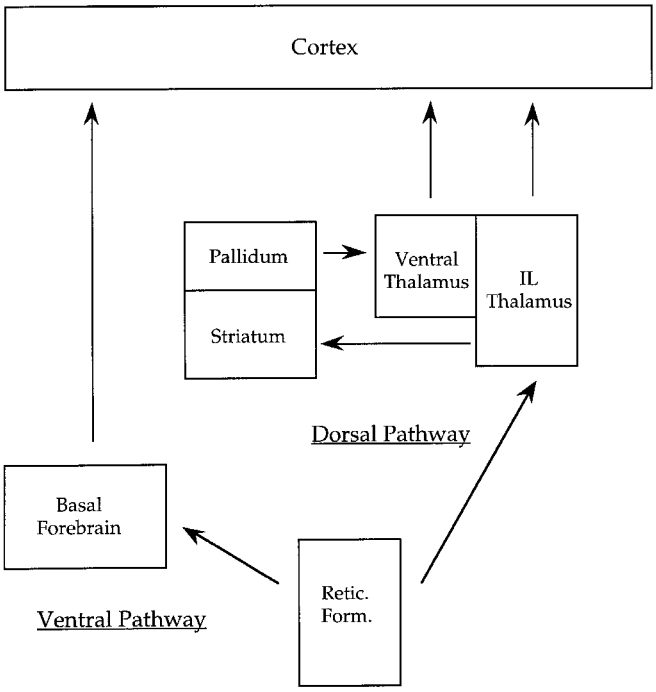

Fig. 6 A schematic diagram illustrating dorsal and ventral pathways of the ascending reticular activating system.

from SWS to REM sleep, while significant, were not as statistically robust as those observed in the midbrain, thalamus, basal forebrain and, in particular, in the basal ganglia.

What function might the basal ganglia have in orchestrating sleep–wake architecture? Our data suggest that these nuclei may in fact play a fundamental role, since changes in striatal activity were the most statistically robust, and in this sense appeared to dominate the transitions from wakefulness to non-REM sleep, and non-REM to REM sleep.

It is not unreasonable to hypothesize a salient role for the basal ganglia in the sleep–wake cycle, for their function is clearly not limited to the motor domain. The basal ganglia appear to be involved in a wide range of attentional, sensory and cognitive processes (Marshall *et al*., 1980; Dunnet, Iversen, 1982; Schneider, 1987) and they also, perhaps via the action of their dopaminergic afferents (Porrino *et al*., 1984; Ongini *et al*., 1985; Monti *et al*., 1988), play a role in regulating levels of behavioural responsiveness and arousal (Kirkby, 1973; Hassler, 1979; McNamara *et al*., 1983). Indeed, early ablation experiments demonstrated that sleep behaviours can be fundamentally, and in some cases permanently, disrupted by lesioning of the striatum and overlying cortex (Villablanca, 1972). Activity of striatal neurons varies systematically throughout the sleep–wake cycle (Moiseeva *et al*., 1969; Sayers and Stille, 1972; Sarkadi *et al*., 1974), and release of acetylcholine in the basal ganglia has been shown to decrease significantly during SWS, and to increase to levels higher than wakefulness during REM sleep (Gadea-Ciria *et al*., 1973).

If the basal ganglia do play a material role in the sleep–wake cycle, what anatomical pathways might subserve these effects? First, the ventral striatum (nucleus accumbens and olfactory tubercle) extends well into, and may represent constituent elements of, the basal forebrain itself (Heimer and Alheid, 1991).

Secondly, as outlined previously, the reticular activating system regulates forebrain activity, in part, via projections to the intralaminar thalamus. Yet, the exact mechanism by which this region of the thalamus exerts its effects upon the cortex has not been established. While direct cortical projections have been demonstrated (Jones and Leavitt, 1974; Royce *et al*., 1989) the basal ganglia are also in a unique position to transmit information from the intralaminar thalamus to the forebrain (Fig. 6). If the density of afferent and efferent projections is an indication of functional significance, this route might indeed be an important one.

The massive projection from intralaminar nuclei to the striatum constitutes the largest efferent outflow from this region of the thalamus (Powell and Cowan, 1956; Sadikot *et al*., 1990) and represents one of the principal afferent inputs to the basal ganglia, as dense as the projections from neocortex (Dray, 1980). In addition to the striatum proper, there are also dense IL thalamic projections to other elements of the basal ganglia core and outflow nuclei (Royce and Mourey, 1985).

The major outflow nuclei of the basal ganglia project, in turn, to the ventral anterior and ventromedial nuclei of the thalamus, projections which are as abundant as the basal ganglia's 'motor' output to the ventrolateral thalamus (Kemp and Powell, 1971; Kim *et al*., 1976; Herkenham, 1979). The ventral anterior and ventromedial nuclei themselves project widely to the entire cortical mantle. These nonspecific nuclei are, in fact, core elements of a generalized thalamocortical system (Hanbery *et al*., 1954; Herkenham, 1986) which appears to be the final common pathway for the cortical recruiting response (Starzl and Magoun, 1951; Sasaki *et al*., 1970; Sasaki, 1975; Glenn *et al*., 1982), i.e. EEG synchronization similar to that observed during drowsiness and sleep, which can be induced by stimulation of the intralaminar thalamus (Morison and Dempsey, 1942; Phillips *et al*., 1972). In addition, these nonspecific nuclei may mediate EEG desynchronization as well (Steriade, 1981). The basal ganglia are therefore in a position to integrate and gate information passing from the reticular core through the intralaminar thalamus, and thus to facilitate either synchronization or desynchronization of cortical activity.

The basal ganglia are also in a position to regulate activity within the ascending reticular activating system itself. The major outflow nuclei have massive projections back to the intralaminar thalamus as well as to the pontine and mesencephalic reticular formation (Nauta, 1979; McGuiness and Krauthamer, 1980). Thus, the connections between brainstem, intralaminar thalamus and basal ganglia could regulate arousal or attentional tone at multiple levels.

Additionally, connections of the basal ganglia provide a mechanism by which these nuclei might modulate REM sleep. The core nuclei of the basal ganglia, including pallidum, substantia nigra and subthalamic nucleus, each project to the pedunculopontine nucleus, one of the major ascending cholinergic nuclei in the rostral brainstem's reticular formation (Mesulam *et al*., 1983*b*; Mitani *et al*., 1988). The pedunculopontine nucleus is thought to be integrally involved in the initiation of REM sleep and may constitute a final common path for the propagation of PGO spikes (Sakai *et al*., 1976; McCarley and Ito, 1983; Vertes, 1984). The basal ganglia are therefore in position to gate the transfer of PGO waves from the brainstem to the thalamus and forebrain. Furthermore, the pedunculopontine nucleus projects to the intralaminar thalamus as well back to the core nuclei. Thus, processes evolving during REM sleep could readily affect activity within the basal ganglia themselves.

Early research sought a role for the basal ganglia in sleep processes (Moiseeva *et al*., 1969; Sayers and Stille, 1972; Villablanca, 1972; Gadea-Ciria *et al*., 1973; Sarkadi *et al*., 1974). Indeed, the notion that the basal ganglia, through their connections with the intralaminar and nonspecific thalamic nuclei, might mediate the effects of the reticular activating system was once commonly entertained (Hassler, 1964). However, when subsequent studies demonstrated direct (albeit restricted) projections from the intralaminar thalamus to the neocortex (Jones and Leavitt, 1974; Royce and Mourey, 1985; Royce *et al*., 1989) interest in the potential significance of basal ganglia circuitry waned. It is now ignored in most contemporary models of sleep, waking and consciousness.

A role for the basal ganglia in REM sleep was ultimately discounted when it became clear that these nuclei were not essential for maintenance of cyclical phenomena which constitute the REM–non-REM sleep cycle: While it may be strongly influenced by the activity of supratentorial afferents (Callaway *et al*., 1987), the REM sleep oscillator is clearly located in the pontine tegmentum, and REM–non-REM sleep oscillations will persist in the absence of the striatum or other core nuclei of the basal ganglia (Siegel, 1985).

However, our results suggest that the search for a material role for the basal ganglia in sleep might be appropriately resurrected. Although fundamental oscillations will persist in their absence, the basal ganglia may be responsible for orchestrating the downstream, supratentorial effects set in motion by the simple change-of-state 'switches' in the brainstem, choreographing within the forebrain, the impact of processes initiated in the centrencephalic core.

Paralimbic and limbic structures

We found that rCBF in paralimbic areas of the brain was systematically related to changes in the state of consciousness (Tables 1–3; Figs 3 and 4). State-dependent activation or deactivation of these regions was seen in all wake–sleep or sleep-stage comparisons, including the contrast between pre- and post-sleep wakefulness. In general, these changes were as robust as those observed in centrencephalic regions.

Limbic core structures, such as amygdala and hippocampus, play an direct role in the expression of drive and affect, and in the homeostatic control of autonomic and endocrine function (Brodal, 1981). Paralimbic regions, such as parahippocampal gyrus, anterior insula, temporal polar and anterior cingulate cortices, on the other hand, are areas of

transitional cortex which serve as a site of information exchange between neocortex and the limbic system proper, thus serving as an interface between the external and internal milieus (Mesulam, 1985).

During deep non-REM sleep, activity in the hippocampus and amygdala did not change (compared with pre-sleep wakefulness), while activity in paralimbic structures decreased dramatically, i.e. rCBF rates in the anterior insula, temporal polar and anterior cingulate cortices were at their nadir during this stage. This suggests that during non-REM sleep, the limbic core structures may be functionally disconnected from brain regions which directly mediate their interactions with the external environment. The notion that non-REM sleep may serve a homeostatic or restorative function is well established (Steriade, 1992; Horne, 1988), and it is possible that a state in which limbic structures are effectively disengaged from the external milieu could be a precondition for such recuperation. The disengagement of vegetative or endocrine machinery might also serve as a diathesis in which internally generated events, such as the phasic secretion of growth hormone during SWS (Takahashi *et al*., 1968), or the restoration of wakefulness-depleted neuronal glycogen stores (Benington and Heller, 1995) can occur.

REM sleep, on the other hand, was associated with profound activation of both the paralimbic belt and the limbic core. Increases in rCBF in lateral paralimbic regions derived from paleocortex (temporal polar and anterior insular cortex), while significant, were not as statistically robust as those in medial regions derived from archicortex (hippocampus, parahippocampal gyri and anterior cingulate cortex).

The potential function of limbic activation during REM sleep is not clear, but is phenomenologically consistent with the autonomic activation and lability observed during REM sleep (Hobson, 1969), and could be related to the rich emotional content of dreams reported during this sleep stage. In addition, activation of the hippocampus–parahippocampal system could be related to the purported impact of REM sleep on memory processes (Crick, and Mitchison, 1983; Smith, 1985; Karni *et al*., 1994), or amnesia for REM sleep-related phenomena *per se* (Goodenough *et al*., 1965).

What physiological processes might account for the deactivation of paralimbic structures during SWS, and their subsequent reactivation during REM sleep? Immuno-histochemical studies suggest a potential mechanism. The paralimbic cortices are the recipient of a rich cholinergic innervation by basal forebrain structures, more dense than the cholinergic projections from basal forebrain to neocortex (Mesulam *et al*., 1983*a*; Rye *et al*., 1984). The changes in synaptic tone within the paralimbic belt might therefore be driven by the robust state-dependent changes in basal forebrain activity. In addition, paralimbic regions project back to the basal forebrain, so the effects might be reciprocal, constituting arousal mechanisms which feed forward upon themselves.

A recently published $H_2{}^{15}O$-PET study (Maquet *et al*., 1996) reported REM sleep-associated increases in rCBF in limbic–paralimbic structures which were in some cases identified (anterior cingulate cortex) and in some cases not (amygdala) in the present study. However, that study contrasted REM sleep scans with all non-REM sleep data obtained, i.e. combining SWS and wakeful-state scans data, whereas we employed state-specific contrasts. The two studies may therefore not be directly comparable.

Neocortical regions

The results of previous PET studies have suggested that non-REM sleep is characterized by a homogeneous decrease in metabolism in the neocortex, and thus a global decrease in cortical synaptic activity (Heiss *et al*., 1985; Maquet *et al*., 1990). Our results reveal that the situation may be more complex. The changes in CBF we observed in the neocortex were not uniform, but were markedly heterogeneous, differing conspicuously in higher order frontoparietal association areas and unimodal occiptotemporal sensory cortices (Table 1; Fig. 3). This functional dissociation, which was manifest at sleep onset and persisted throughout the sleep–wake cycle (including REM sleep; Tables 2 and 3), may be a defining characteristic of sleep itself.

During normal awake consciousness, the prefrontal cortices perform the highest order processing of neural information, integrating sensory, cognitive and limbic information, organizing meaningful, temporally sequenced behavioural responses and subserving working memory. The inferior parietal cortices are involved in cross-modal association of perceptual material necessary for higher cortical activities such as language. The onset of non-REM sleep was associated with dramatic and specific deactivation of these regions.

Activity levels in post-rolandic unimodal sensory cortices, on the other hand, were preserved during SWS. These regions are involved in lower level processing of modality-specific information and serve as an obligatory relay for the transfer of this information to other regions of the brain. Our results suggest that these areas may possibly be characterized by a minimum, perhaps self-generating, level of activity below which they will not drop, i.e. an effective ‘floor effect’, during non-REM sleep.

Taken together, these data indicate that regions constituting the first cortical relay for exteroceptive stimuli may remain active or ‘alert’ during SWS, but are dissociated from regions ‘downstream’ with which they are functionally coupled during wakefulness. In other words, while primary and secondary sensory areas may remain active during SWS, the higher order association cortices to which they project, regions in which sensation acquires a larger meaning, are relatively silent.

A similar functional dissociation was observed in more primitive proisocortical regions to which the frontoparietal and occipitotemporal cortices project. Activity in the anterior portion of the insula, paralimbic cortex associated with the prefrontal system, decreased during SWS (Table 1; Fig. 3),

while the posterior portion of the insula, functionally associated with post-rolandic unimodal sensory cortices, remained active (Mesulam and Mufson, 1986). Similarly, activity in the anterior cingulate, which is functionally related to the prefrontal cortex and plays an associative or executive role, decreased during SWS; activity in the posterior cingulate, which is more closely related to post-rolandic unimodal sensory systems and serves a sensory or evaluative function (Vogt *et al*., 1992), remained unchanged (Table 1; Fig. 3).

What mechanisms might account for the focal deactivation of frontoparietal association areas and preservation of activity in the unimodal sensory cortices? The non-uniform cortical projections of the intralaminar thalamus may play a role. Direct projections from intralaminar thalamus are more abundant in the frontal and parietal association areas, while projections to the unimodal visual and auditory regions are relatively sparse (Kaufman and Rosenquist, 1985; Macchi and Bentivoglio, 1986; Berendse and Groenewegen, 1991); cortical recruiting responses induced by stimulation of the intralaminar thalamus appear to be restricted to frontal, cingulate and posterior suprasylvian areas, and are absent in the unimodal sensory cortical regions (Starzl and Magoun, 1951; Sasaki, 1975). Thus, attenuated activation of the intralaminar thalamus by the brainstem reticular formation during non-REM sleep might be expected to have a disproportionate effect on the frontoparietal regions, perhaps 'sparing' the occipitotemporal cortices.

However, it is not likely that synaptic activity in the unimodal sensory areas is maintained by ongoing thalamic transmission of sensory information from the periphery, because the sensory relay nuclei of the thalamus are inactive during SWS as well. It is more likely that unimodal sensory activity is preserved within local circuitry or represents intracortical or transcollosal transfer of information.

What function, if any, might be served by the persistence of activity in post-rolandic sensory fields during non-REM sleep? It may simply be that the maintenance of synaptic activity reflects a relatively low need for recuperative benefits of SWS in these regions compared with that of the higher order association cortices. On the other hand, persistence of post-rolandic cortical synaptic activity may keep these systems prepared or 'primed' for sudden arousal. There may be adaptive or survival value associated with sustaining an essential level of activity which would enhance effective functioning when thalamocortical activity is re-established. This would be particularly true when waking occurs rapidly, in response to a sudden threat from the environment.

Persistence of activity in the unimodal sensory cortices may play a role in stimulus-induced arousal itself. That is, this activity may support a discriminative function at the level of the secondary sensory cortices themselves, permitting an individual in this sleep stage to evaluate the salient features of a stimulus. Consistent with this notion, it has been shown that the presentation of one's own name will result in behavioural and electroencephalographic arousal, whereas presentation of comparably loud, but less meaningful, stimuli will not (Langford *et al*., 1974).

The functional dissociation between activity in fronto-parietal and occipitotemporal systems persisted during REM sleep (Tables 2 and 3). There were marked increases in activity in discrete post-rolandic cortical areas during REM sleep, more prominent in secondary than in primary sensory cortices, and most pronounced in the auditory and visual systems. The marginal differences which were detected in somatosensory and somatomotor regions might be due to greater inter-subject variability in the activity of peri-rolandic structures (the largest coefficients of variation were observed in peri-rolandic regions in all stages of sleep), or to the reduced sample space, i.e. a relative undersampling of Brodmann areas 5 and 7, the lateral premotor cortex and supplementary motor area. Similarly, the frontal eye fields (Brodmann area 8, superior dorsolateral prefrontal cortex), where changes in rCBF might be expected to subserve eye movements associated with REM sleep, were not adequately sampled in the majority of subjects.

Within the temporal and occipital cortices, however, REM sleep-induced increases in rCBF were conspicuous. The rCBF was significantly increased in visual association areas (Brodmann area 19, 37), as well as the anterior auditory association areas (Brodmann area 22, although increases were not as robust there as in the visual areas).

In contrast to the REM sleep-related activation of these post-rolandic sensory cortices, heteromodal areas including the dorsolateral prefrontal cortex, lateral orbital cortex and inferior parietal lobule (each of which was deactivated at the onset of non-REM sleep) remained inactive during REM sleep. Similarly, activity in the heteromodal portions of the temporal lobe, i.e. the anterior middle temporal gyrus and superior temporal sulcus, did not increase during REM (versus non-REM) sleep.

Increased activity in the visual cortex and decreased activity in the inferior prefrontal regions observed in the present study are consistent with the results of a previous SPECT study of REM sleep (Madsen *et al*., 1991*a*), and decreased rCBF in prefrontal areas during REM sleep has been reported in a recent PET study as well (Maquet *et al*., 1996). The present results, however, suggest that changes observed during REM sleep are part of a larger and more comprehensive pattern of brain activity which is manifest throughout the course of the sleep–wake cycle:

As illustrated in Fig. 7, the onset of SWS was associated with decreases in neuronal activity in all brain regions, with the exception of the unimodal, post-rolandic sensory cortices (typified in this case by the auditory cortices of the superior temporal gyrus). The most precipitous decreases in the neocortex were found in the heteromodal regions, i.e. the prefrontal cortex and inferior parietal lobule (*see* also Fig. 3). Deactivation of the heteromodal cortices may be a constituent feature of sleep itself; during REM sleep (Figs 4 and 7), while rCBF in centrencephalic, paralimbic, limbic and unimodal sensory regions increased, activity in the prefrontal and

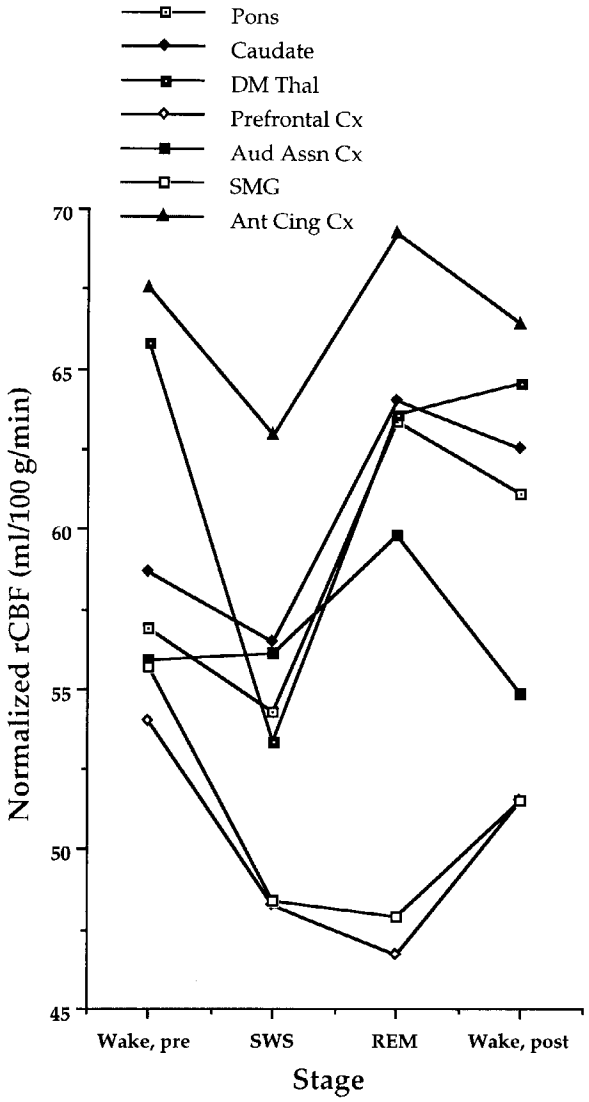

Fig. 7 Line graph illustrating changes in rCBF in selected centrencephalic, paralimbic and neocortical regions of interest throughout the sleep–wake cycle. Values are normalized, averaged and scaled as outlined in the Material and methods section. Talairach coordinates used to extract regional data from individual PET scans are as follows: pons, $x = \pm 4$, $y = -32$, $z = -28$; caudate, $x = \pm 7$, $y = 13$, $z = 0$; dorsomedial (DM) thalamus, $x = \pm 7$, $y = -15$, $z = 8$; prefrontal cortex, $x = \pm 44$, $y = 40$, $z = 0$; auditory association cortex, $x = \pm 5$, $y = 31$, $z = 0$; supramarginal gyrus (SMG), $x = \pm 47$, $y = -44$, $z = 40$; anterior cingulate cortex, $x = \pm 9$, $y = 41$, $z = 8$.

inferior parietal cortices remained depressed, increasing only at the onset of wakefulness (Figs 5 and 7). In other words, REM sleep may consititute a state of generalized brain activity with the specific exclusion of executive systems which normally participate in the highest order analysis and integration of neural information.

In contrast while dorsolateral prefrontal and lateral orbital cortices remained inactive, rCBF in the medial prefrontal cortices, the prefrontal area with the richest limbic connections (Damasio and Anderson, 1993; Partiot *et al.*, 1995), increased significantly during REM sleep to levels above those detected during either SWS or wakefulness (Tables 2 and 3; Fig. 3), although these increases were not as statistically robust as those in the sensory areas.

While not as intensively studied at this point as the lateral convexities, the medial prefrontal cortices appear to subserve functions which may be related to REM sleep. They are functionally related to the mesencephalic activation system (Luria, 1980), and are clearly involved with processes of arousal and attention (Cummings, 1985). In addition, structural lesions within this region can produce confabulation, the impulsive production of fabricated information, unbridled by reason or social context, in patients with amnesia (Benson *et al.*, 1996). Thus, participation of the medial prefrontal cortex could be related to the bizarre, albeit uncritically experienced narrative imagery of dreams.

Cortical–subcortical interactions in REM and non-REM sleep

The thalamus and cortex have evolved in close relationship with one another in the course of vertebrate evolution, and the thalamic nuclei and the cortical regions with which they are interconnected may be considered as functionally contingent systems. Viewed in this way, the evaluation of cortico-thalamic interactions during the sleep–wake cycle may be more revealing than the study of either element independently.

In the transition from wakefulness to non-REM sleep, decreased activity in the dorsolateral prefrontal and lateral orbital regions was matched by a corresponding reduction in the dorsomedial nucleus of the thalamus, with which these cortical areas are reciprocally connected (Table 1). Thus, the prefrontal cortex –dorsomedial thalamic system appeared to be deactivated in a coherent manner. Similarly, parahippocampal cortex, anterior cingulate cortex and the anterior nucleus of the thalamus appeared to be deactivated as a system during non-REM sleep (Table 1).

In contrast, sensory nuclei of the thalamus, i.e. pulvinar, geniculate, and ventral posterior areas, were deactivated while activity levels in post-rolandic sensory cortices did not change (Table 1). In other words, the sensory thalamus and related regions of the neocortex appear to be ‘uncoupled’ at sleep onset. On the other hand, in the transition from non-REM to REM sleep (Table 2), prominent increases in activity in the sensory thalamus were matched by increases in portions of the occipital and temporal cortices. This suggests that the sensory thalamus and neocortex may become functionally ‘recoupled’ during REM sleep.

Communication between the sensory thalamus and cerebral cortex may be necessary to bind together sensory information reaching the brain in a manner that is experienced as consciousness (Joliot *et al.*, 1994; Pare and Llinas, 1995). The breach of coherence in this thalamocortical system may be a defining property of ‘unconsciousness’ which is

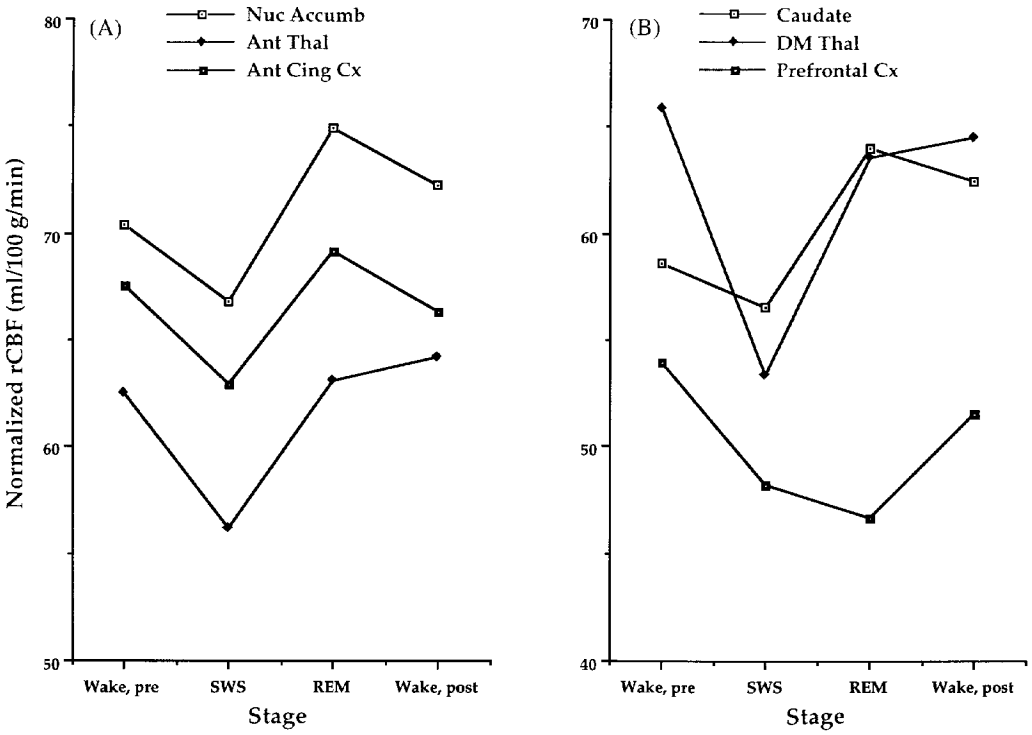

Fig. 8 Line graph illustrating changes in rCBF in elements of (**A**) limbic and (**B**) prefrontal corticostriatal–thalamocortical circuits throughout the sleep–wake cycle. Values are normalized, averaged and scaled as outlined in Material and Methods section. Talairach coordinates used to extract regional data from individual PET scans are as follows: nucleus accumbens, $x = \pm 10$, $y = 8$, $z = -8$; anterior thalamus, $x = \pm 8$, $y = -7$, $z = 8$; anterior cingulate cortex, $x = \pm 9$, $y = 41$, $z = 8$; caudate, $x = \pm 7$, $y = 13$, $z = 0$; dorsomedial (DM) thalamus, $x = \pm 7$, $y = -15$, $z = 8$; prefrontal cortex, $x = \pm 44$, $y = 40$, $z = 0$.

characteristic of non-REM sleep, as opposed to REM sleep or wakefulness.

Relationships of cortical and subcortical regions can be looked at in another way, by considering the concurrent activity of cortex, thalamus and basal ganglia. It has been proposed (Alexander *et al*., 1986; Parent and Hazrati, 1995), that there are multiple, parallel circuits connecting functionally related regions of the striatum, thalamus and frontal or cingulate cortices, the so-called corticostriatal–thalamocortical loops.

Our findings suggest that, in general, these circuits, e.g. the 'limbic' loop connecting ventral striatum, anterior thalamus and paralimbic cortices, appear to be activated in an integrated fashion during REM sleep (Table 2; Fig. 8A). However, the prefrontal or 'association' loop, connecting the caudate, dorsomedial thalamus and prefrontal cortices (Table 2; Fig. 8B), appears to be activated only in a partial or fragmentary way.

Significant increases in rCBF were detected in both dorsal and ventromedial portions of the caudate (they are, in fact, the most statistically robust increases observed during REM sleep), while activity in the dorsolateral prefrontal and lateral orbital cortices did not change. Thus, during REM sleep, the caudate may be operating in a 'stand-alone' mode, independent of activity in its primary source of neocortical afferents.

It is not likely that this represents spontaneous activity of intrinsic striatal neurons, since, at least during wakefulness, most of these neurons are silent until extrinsically activated (Richardson *et al*., 1977; Wilson, 1990). A likely source of such extrinsic input during REM sleep would be the intralaminar thalamus (Fig. 9, number 4) which, as noted above, is the source of a massive projection by which information may be transferred from the reticular activating system to the basal ganglia (Powell and Cowan, 1956; Sadikot *et al*., 1990). In fact, it has been proposed that the intralaminar thalamus might 'gate' or selectively activate the various corticostriatal–thalamocortical circuits (Groenewegen and Berendse, 1994); such selective activation might, in part, shape the regional activations manifest during REM sleep.

What might be the functional significance of the fragmented activation of the prefrontal circuit during REM sleep? It is possible that this reflects a 'systems check' and/or alerting function of REM sleep. Our results suggest that deactivation of the lateral orbital and dorsolateral prefrontal cortices, the single most salient feature common to both non-REM and REM states, may be a defining characteristic of sleep *per se*. Reduced CBF in these regions may be indicative of, or may represent a necessary precondition for, recuperation during sleep. Activation during REM sleep might thus serve as a means of checking the readiness of frontal regions for waking. Activation of the caudate during REM sleep without corresponding activation of the lateral prefrontal cortices and dorsal thalamus (Fig. 9, numbers 1, 2 and 3) might indicate

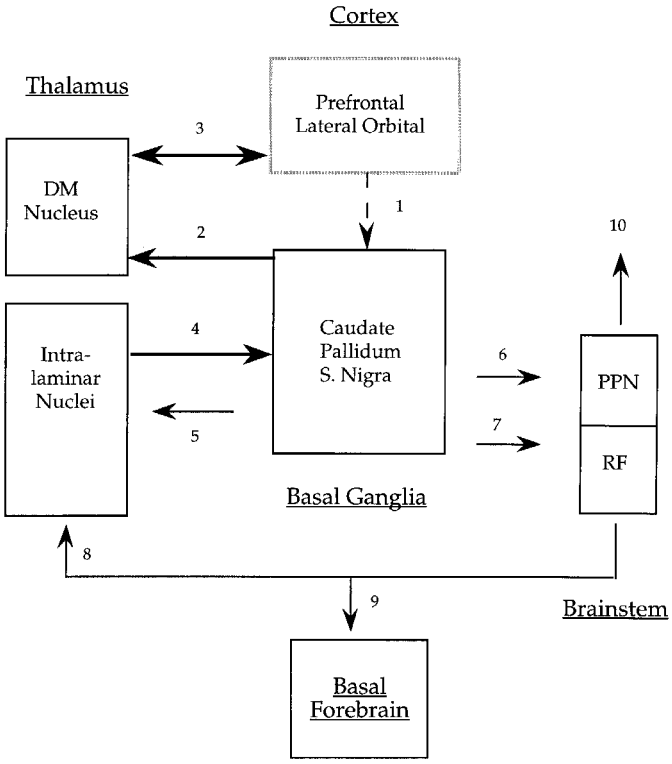

Fig. 9 A schematic illustration of cortical and subcortical connections of the caudate nucleus. DM = dorsomedial thalamic nucleus; PPN = pedunculopontine nucleus; RF = rostral pontine and mesencephalic reticular formation; S. Nigra = substantia nigra.

a need for additional sleep, and ultimately result in the end of the REM sleep period and the re-initiation of SWS. The termination of REM sleep could be brought about by the basal ganglia themselves, mediated by projections from output nuclei to the pedunculopontine nucleus (Fig. 9, number 6), and the reappearance of SWS could be initiated via the dense projections from the output nuclei to the intralaminar thalamus and reticular formation (Fig. 9, numbers 5, 7 and 9).

On the other hand, 'matched' increases in activity in caudate, lateral prefrontal cortex and dorsomedial thalamus, i.e. reintegration of this corticostriatal–thalamocortical circuit, might indicate physiological readiness for wakefulness or it might actually constitute wakefulness in itself. In this case, the degree to which activity in the prefrontal cortex and dorsal thalamus are functionally coupled with activity in the caudate might represent a fundamental difference between REM sleep and normal waking consciousness.

It may be important to note that our data were generally acquired during the first REM sleep episode, and our findings could be biased by this. All of the results we report, including partial integration of the corticostriatal–thalamocortical circuitry, might be characteristic of REM sleep episodes which occur early in the sleep period and may therefore be distinctly different from what would be seen later following several non-REM–REM sleep cycles. If our hypothesis is correct, it might be predicted that REM episodes occurring later in the sleep period would be characterized by increasing coherence of prefrontal, dorsomedial thalamic and striatal activity, which could also underlie the time-of-night dependent changes in the length and complexity of REM sleep dream reports (Snyder, 1970; Cipolli and Poli, 1992). Future studies should include comparison of REM episodes across the sleep period.

Pre- versus post-sleep wakefulness

The most conspicuous differences in the comparison of pre- and post-sleep wakefulness studies were large decreases in absolute pCO_2-corrected blood-flow levels, with global CBF significantly lower during post-sleep than pre-sleep wakefulness (Fig. 2). Indeed, in this contrast, differences in absolute rather than normalized rCBF rates were the more statistically robust (i.e. they generated the largest *Z*-scores), a finding unlike the more typical case, in which normalized comparisons were generally associated with the lower probabilities of error. This suggests a generalized, relatively uniform decrease in CBF following recovery sleep.

The post-sleep wakefulness depression of CBF was not entirely homogeneous, however. The analysis of normalized rCBF identified regionally specific decreases, and ultimately suggests that a dissociation between activity in limbic, paralimbic and neocortical regions on one hand, and centrencephalic regions of interest on the other, may characterize sleep deprivation and/or recovery (Table 4).

There were no apparent differences in the activity of centrencephalic structures, including the basal forebrain, brainstem, basal ganglia and thalamus, when pre- and post-sleep wakefulness studies were compared (Table 4), i.e. positive *Z*-scores indicated a relative invariance in absolute flow rates. Thus, our results suggest that activity in these regions appears to be related to wakefulness *per se*, without differences attributable to sleep deprivation or intervening sleep. Indeed, activity in centrencephalic structures related to arousal might be expected to remain constant in the comparison of wakefulness studies, representing a constituent characteristic of conscious wakefulness.

In contrast, activity in limbic and neocortical regions was clearly affected by the intervening period of sleep. Decreases in activity during post-sleep wakefulness were manifest in post-rolandic unimodal sensory regions, i.e. in the auditory and visual cortices of the temporal and occipital lobes (Table 4), even though activity in these regions did not change during the transition from wakefulness to SWS and increased during REM sleep. Activity in the prefrontal and parietal association cortices was also lower during post-sleep than pre-sleep wakefulness, although activity in these regions had apparently rebounded from the low levels observed during both REM and non-REM sleep. Compared with pre-sleep wakefulness, activity was also reduced in the hippocampus following recovery sleep. Decreases during post-sleep wakefulness were most statistically reliable here and in the inferior and middle temporal gyri.

It is not clear at this point whether such differences actually represent increases in CBF due to sleep deprivation or decreases brought about by the intervening period of recovery sleep (or both). If interpreted as the consequence of sleep deprivation, increased activity in mesial temporal and neocortical regions might represent the functional correlates of hypnogenic processes which precede sleep onset. However, if interpreted as changes due to the effect of recovery sleep, decreased activity in limbic and neocortical structures may reflect recuperative or restorative effects of sleep, manifest at the onset of wakefulness.

An abrupt reduction in CBF upon waking, although somewhat paradoxical, would not be entirely unexpected. As noted above, a previous study (Hajak *et al*., 1994) reported rapid reductions in cerebral arterial blood flow immediately following waking from sleep. Furthermore, changes observed in that study represented decreases from values measured during both non-REM sleep and pre-sleep wakefulness, at which time subjects were *not* sleep-deprived. These findings suggest that the differences we observed might reflect a physiological consequence of arousal from recovery sleep more accurately than the effects of sleep deprivation.

Nevertheless, it should be mentioned that, in the absence of fully rested, midday baseline data, all of the differences we report here might represent, at least in part, functional changes related to sleep deprivation. That is, it is possible that subjects failed to obtain adequate recovery sleep in the PET scanner, and were still relatively 'sleep deprived' upon waking at the end of the scanning session. Further investigations will be necessary in which non-sleep-deprived subjects are studied prior to, and following, an adequate period of recovery sleep. Similarly, potential circadian effects on sleep–wake architecture were not systematically excluded in the present study, and future investigations should evaluate rCBF patterns associated with sleep during different portions of the circadian cycle. Finally, it should be stressed that this was an exploratory study, which evaluated a large number of regional variables, and was undertaken to generate rather than test hypotheses; the results will need to be replicated.

Conclusions

The comparisons of wakefulness, SWS and REM sleep reveal that fundamental, state-dependent changes in the functional organization of the brain occur during the course of the human sleep–wake cycle.

Centrencephalic structures appear to play an integral role in the genesis of each sleep or wakefulness state. The state-dependent changes detected in the brainstem, thalamus and basal forebrain are consistent with previous studies which have demonstrated the involvement of these structures in systems mediating arousal. The shifts in the level of activity of the striatum represent the most significant changes detected in comparisons of wakefulness, SWS and REM sleep. The basal ganglia may be more integrally involved in the orchestration of the sleep–wake cycle than previously thought.

State-dependent differences in the activity of limbic and paralimbic regions paralleled those observed in centrencephalic structures, and differentiated pre- and post-sleep wakefulness states as well. This suggests that limbic and paralimbic areas play a significant role in all state transitions. Variations in the activity of these regions may relate to the affective, emotional, autonomic and endocrine phenomena associated with both REM and non-REM sleep.

Significant, regionally heterogeneous differences in neocortical activity constituted a salient feature of each sleep stage. A functional dissociation between activity in frontoparietal association and post-rolandic unimodal sensory areas appears to be characteristic of both REM and non-REM sleep. SWS is associated with selective deactivation of higher order frontoparietal association areas and preservation of activity in primary and secondary sensory cortices. REM sleep is characterized by selective activation of certain unimodal sensory cortices (along with centrencephalic, paralimbic and limbic regions of the brain) to the exclusion of frontoparietal association systems. That is, REM sleep appears to represent a generalized activation of the brain without the participation of regions normally responsible for the highest order analysis and integration of neural information. Deactivation of the heteromodal association areas represents the single feature common to both non-REM and REM states, and may be a defining characteristic of sleep itself.

Altered relationships between cortical and subcortical brain regions appear to differentiate the various stages of sleep. SWS is characterized by what may be a functional disconnection of thalamic relay nuclei and post-rolandic sensory cortices. REM sleep may be characterized by a partial or fragmented activation of corticostriatal–thalamocortical association circuitry. The difference between activation during REM sleep and activation during normal waking consciousness might be the degree to which the lateral prefrontal cortex and dorsomedial thalamus are functionally coupled with associated regions of the basal ganglia.

References

Alexander GE, DeLong MR, Strick PL. Parallel organization of functionally segregated circuits linking basal ganglia and cortex. [Review]. Annu Rev Neurosci 1986; 9: 357–81.

Asenbaum S, Zeitlhofer J, Saletu B, Frey R, Brucke T, Podreka I, et al. Technetium-99m-HMPAO SPECT imaging of cerebral blood flow during REM sleep in narcoleptics. J Nucl Med 1995; 36: 1150–5.

Benington JH, Heller HC. Restoration of brain energy metabolism as the function of sleep. [Review]. Prog Neurobiol 1995; 45: 347–60.

Benson DF, Djenderedjian A, Miller BL, Pachana NA, Chang L, Itti L, et al. Neural basis of confabulation. Neurology 1996; 46: 1239–43.

Berendse HW, Groenewegen HJ. Restricted cortical termination

fields of the midline and intralaminar thalamic nuclei in the rat. Neuroscience 1991; 42: 73–102.

Bremer F. Cerveau 'isole' et physiologie du sommeil. C R Soc Biol (Paris) 1935; 118: 1235–41.

Brodal A. The cerebellum. In Brodal A. Neurological anatomy. 3rd ed. New York: Oxford University Press, 1981: 294–393.

Buchsbaum MS, Gillin JC, Wu J, Hazlett E, Sicotte N, Dupont RM, et al. Regional cerebral glucose metabolic rate in human sleep assessed by positron emission tomography. Life Sci 1989; 45: 1349–56.

Callaway CW, Lydic R, Baghdoyan HA, Hobson JA. Pontogeniculooccipital waves: Spontaneous visual system activity during rapid eye movement sleep. [Review]. Cell Moll Neurobiol 1987; 7: 105–49.

Cipolli C, Poli D. Story structure in verbal reports of mental sleep experience after awakening in REM sleep. Sleep 1992; 15: 133–42.

Crick F, Mitchison G. The function of dream sleep. Nature 1983; 304: 111–4.

Cummings JL. Clinical neuropsychiatry. Orlando (FL): Grune & Stratton, 1985: 57–67.

Damasio AR, Anderson SW. The frontal lobes. In: Heilman KM, Valenstein E, editors. Clinical neuropsychology. 3rd ed. New York: Oxford University Press, 1993: 409–60

Douglas J, White DP, Pickett CK, Weil JV, Zwillich CW. Respiration during sleep in normal man. Thorax 1982; 37: 840–4.

Dray A. The physiology and pharmacology of mammalian basal ganglia. [Review]. Prog Neurobiol 1980; 14: 221–335.

Dunnett SB, Iversen SD. Sensorimotor impairments following localized kainic acid and 6-hydroxydopamine lesions of the neostriatum. Brain Res 1982; 248: 121–7.

Fox PT, Mintun MA, Raichle ME, Miezin FM, Allman JM, Van Essen DC. Mapping human visual cortex with positron emission tomography. Nature 1986; 323: 806–809.

Franzini C. Brain metabolism and blood flow during sleep. J Sleep Res 1992; 1: 3–16.

Friston KJ, Passingham RE, Nutt JG, Heather JD, Sawle GV, Frackowiak RSJ. Localisation in PET images: direct fitting of the intercommissural (AC-PC) line. J Cereb Blood Flow Metab 1989; 9: 690–5.

Friston KJ, Frith CD, Liddle PF, Dolan RJ, Lammertsma AA, Frackowiak RSJ. The relationship between global and local changes in PET scans. J Cereb Blood Flow Metab 1990; 10: 458–66.

Friston KJ, Frith CD, Liddle PF, Frackowiak RSJ. Comparing functional (PET) images: the assessment of significant change. J Cereb Blood Flow Metab 1991; 11: 690–9.

Fuller JH. Brain stem reticular units: some properties of the course and origin of the ascending trajectory. Brain Res 1975; 83: 349–67.

Gadea-Ciria M, Stadler H, Lloyd KG, Bartholini G. Acetylcholine release within the cat striatum during the sleep-wakefulness cycle. Nature 1973; 243: 518–9.

Glenn LL, Hada J, Roy JP, Deschenes M, Steriade M. Anterograde tracer and field potential analysis of the neocortical layer I projection from nucleus ventralis medialis of the thalamus in cat. Neuroscience 1982; 7: 1861–77.

Goodenough DR, Lewis HB, Shapiro A, Sleser I. Some correlates of dream reporting following laboratory awakenings. J Nerv Ment Dis 1965; 140: 365–73.

Groenewegen HJ, Berendse HW. The specificity of the 'nonspecific' midline and intralaminar thalamic nuclei. [Review]. Trends Neurosci 1994; 17(2): 52–7.

Hajak G, Klingelhöfer J, Schulz-Varszegi M, Matzander G, Sander D, Conrad B, et al. Relationship between cerebral blood flow velocities and cerebral electrical activity in sleep. Sleep 1994; 17: 11–9.

Hanbery J, Ajmone-Marsan C, Dilworth M. Pathways of non-specific thalamo-cortical projection system. Electroencephalogr Clin Neurophysiol 1954; 6: 103–18.

Hassler R. Spezifische und unspezifische Systeme des menschlichen Zwischenhirns. Prog Brain Res 1964; 5: 1–32.

Hassler R. Striatal regulation of adverting and attention directing induced by pallidal stimulation. Appl Neurophysiol 1979; 42: 98–102.

Heimer L, Alheid GF. Piecing together the puzzle of basal forebrain anatomy. In: Napier TC, Kalivas PW, Hanin I, editors. The basal forebrain. Advances in experimental medicine and biology, Vol. 295. New York: Plenum Press, 1991: 1–42.

Heiss WD, Pawlik G, Herholz K, Wagner R, Wienhard K. Regional cerebral glucose metabolism in man during wakefulness, sleep, and dreaming. Brain Res 1985; 327: 362–6.

Herkenham M. The afferent and efferent connections of the ventromedial thalamic nucleus in the rat. J Comp Neurol 1979; 183: 487–517.

Herkenham M. New perspectives on the organization and evolution of nonspecific thalamocortical projections. In: Jones EG, Peters A, editors. Cerebral cortex, Vol. 5. New York: Plenum Press, 1986: 403–45.

Hobson JA. Sleep: physiologic aspects. [Review]. N Engl J Med 1969; 281: 1343–5.

Hong CC-H, Gillin JC, Dow BM, Wu J, Buchsbaum MS. Localized and lateralized cerebral glucose metabolism associated with eye movements during REM sleep and wakefulness: A positron emission tomography (PET) study. [Review]. Sleep 1995; 18: 570–80.

Horne J. Why we sleep: the functions of sleep in humans and other mammals. Oxford: Oxford University Press, 1988.

Jasper H. Diffuse projection systems: the integrative action of the thalamic reticular system. Electroencephalogr Clin Neurophysiol 1949; 1: 405–20.

Joliot M, Ribary U, Llinas R. Human oscillatory brain activity near 40 Hz coexists with cognitive temporal binding. Proc Natl Acad Sci USA 1994; 91: 11748–51.

Jones EG, Leavitt RY. Retrograde axonal transport and the demonstration of non-specific projections to the cerebral cortex and striatum from thalamic intralaminar nuclei in the rat, cat and monkey. J Comp Neurol 1974; 154: 349–77.

Jueptner M, Weiller C. Review: Does measurement of regional cerebral blood flow reflect synaptic activity? – Implications for PET and fMRI. Neuroimage 1995; 2: 148–56.

Kanai T, Szerb JC. Mesencephalic reticular activating system and cortical acetylcholine output. Nature 1965; 205: 80–2.

Karni A, Tanne D, Rubenstein BS, Askenasy JJM, Sagi D. Dependence on REM sleep of overnight improvement of a perceptual skill [see comments]. Science 1994; 265: 679–82. Comment in: Science 1994; 265: 603–4.

Kaufman EF, Rosenquist AC. Afferent connections of the thalamic intralaminar nuclei in the cat. Brain Res 1985; 335: 281–96.

Kemp JM, Powell TPS. The connexions of the striatum and globus pallidus: synthesis and speculation. Philos Trans R Soc Lond B Biol Sci 1971; 262: 441–57.

Kim R, Nakano K, Jayaraman A, Carpenter MB. Projections of the globus pallidus and adjacent structures: an autoradiographic study in the monkey. J Comp Neurol 1976; 169: 263–90.

Kirkby RJ. Caudate nucleus and arousal in the rat. J Comp Physiol Psychol 1973; 85: 82–96.

Koeppe RA, Holden JE, Ip WR. Performance comparison of parameter estimation techniques for the quantitation of local cerebral blood flow by dynamic positron computed tomography. J Cereb Blood Flow Metab 1985; 5: 224–34.

Langford GW, Meddis R, Pearson AJD. Awakening latency from sleep for meaningful and non-meaningful stimuli. Psychophysiology 1974; 11: 1–5.

Luria AR. Higher cortical funtions in man. New York: Basic Books, 1980.

Macchi G. Bentivoglio M. The thalamic intralaminar nuclei and the cerebral cortex. In: Jones EG, Peters A, editors. Cerebral cortex, Vol. 5. New York: Plenum Press, 1986: 355–401.

Madsen PL. Blood flow and oxygen uptake in the human brain during various states of sleep and wakefulness. [Review]. Acta Neurol Scand Suppl 1993; 148: 3–27.

Madsen PL, Vorstrup S. Cerebral blood flow and metabolism during sleep. [Review]. Cerebrovasc Brain Metab Rev 1991; 3: 281–96.

Madsen PL, Holm S, Vorstrup S, Friberg L, Lassen NA, Wildschiodtz G. Human regional cerebral blood flow during rapid-eye-movement sleep. J Cereb Blood Flow Metab 1991a; 11: 502–7.

Madsen PL, Schmidt JF, Wildschiodtz G, Friberg L, Holm S, Vorstrup S, et al. Cerebral O2 metabolism and cerebral blood flow in humans during deep and rapid-eye-movement sleep. J Appl Physiol 1991b; 70: 2597–601.

Mangold R, Sokoloff L, Conner E, Klienerman J, Therman PG, Kety SS. The effects of sleep and lack of sleep on the cerebral circulation and metabolism of normal young men. J Clin Invest 1955; 34: 1092–00.

Maquet P, Dive D, Salmon E, Sadzot B, Franco G, Poirrier R, et al. Cerebral glucose utilization during sleep-wake cycle in man determined by positron emission tomography and [18F] 2-fluoro-2-deoxy-D-glucose method. Brain Res 1990; 513: 136–43.

Maquet P, Peters J-M, Aerts J, Delfiore G, Degueldre C, Luxen A, et al. Functional neuroanatomy of human rapid-eye-movement sleep and dreaming [letter]. Nature 1996; 383: 163–6.

Marshall JF, Berrios N, Sawyer S. Neostriatal dopamine and sensory inattention. J Comp Physiol Psychol 1980; 94: 833–46.

McCarley RW, Hobson JA. Single neuron activity in cat gigantocellular tegmental field: selectivity of discharge in desynchronized sleep. Science 1971; 174: 1250–2.

McCarley RW, Ito K. Intracellular evidence linking medial pontine reticular formation neurons to PGO wave generation. Brain Res 1983; 280: 343–8.

McGuinness CM, Krauthamer GM. The afferent projections to the centrum medianum of the cat as demonstrated by retrograde transport of horseradish peroxidase. Brain Res 1980; 184: 255–69.

McNamara JO, Rigsbee LC, Galloway MT. Evidence that substantia nigra is crucial to neural network of kindled seizures. Eur J Pharmacol 1983; 86: 485–6.

Mesulam MM. Patterns in behavioral neuroanatomy: association areas, the limbic system, and hemispheric specialization. In: Mesulam MM. Principles of behavioral neurology. Philadelphia: F.A. Davis, 1985: 1–70.

Mesulam MM. Mufson EJ. The insula of Reil in man and monkey. In: Peters A, Jones EG, editors. Cerebral cortex, Vol. 4. New York: Plenum Press, 1986: 179–226.

Mesulam MM, Mufson EJ, Levey AI, Wainer BH. Cholinergic innervation of cortex by the basal forebrain: Cytochemistry and cortical connections of the septal area, diagonal band nuclei, nucleus basalis (substantia innominata), and hypothalamus in the rhesus monkey. J Comp Neurol 1983a; 214: 170–97.

Mesulam MM, Mufson EJ, Wainer BH, Levey AI. Central cholinergic pathways in the rat. Neuroscience 1983b; 10: 1185–201.

Mitani A, Ito K, Hallanger AE, Wainer BH, Kataoka K, McCarley RW, et al. Cholinergic projections from the laterodorsal and pedunculopontine tegmental nuclei to the pontine gigantocellular tegmental field in the cat. Brain Res 1988; 451: 397–402.

Moiseeva NI, Movissiants SA, Trohatchev AI. Characteristics of bioelectrical events in subcortical structures during different phases of sleep in man. Electroencephalogr Clin Neurophysiol 1969; 27: 698.

Monti JM, Hawkins M, Jantos H, D'Angelo L, Fernandez M. Biphasic effects of dopamine D-2 receptor agonists on sleep and wakefulness in the rat. Psychopharmacology (Berl) 1988; 95: 395–400.

Morison RS, Dempsey EW. A study of thalamo-cortical relations. Am J Physiol 1942; 135: 281–92.

Moruzzi G, Magoun HW. Brain stem reticular formation and activation of the EEG. Electroencephalogr Clin Neurophysiol 1949; 1: 455–73.

Munk MHJ, Roelfsema PR, Konig P, Engel AK, Singer W. Role of reticular activation in the modulation of intracortical synchronization [see comments]. Science 1996; 272: 271–4. Comment in: Science 1996; 272: 225–6.

Nauta HJ. Projections of the pallidal complex: an autoradiographic study in the cat. Neuroscience 1979; 4: 1853–73.

Ongini E, Caporali MG, Massotti M. Stimulation of dopamine D-1 receptors by SKF 38393 induces EEG desynchronization and behavioral arousal. Life Sci 1985; 37: 2327–33.

Pare D, Llinas R. Conscious and pre-conscious processes as seen from the standpoint of sleep-waking cycle neurophysiology. [Review]. Neuropsychologia 1995; 33: 1155–68.

Parent A, Hazrati LN. Functional anatomy of the basal ganglia. I. The cortico-basal ganglia-thalamo-cortical loop. [Review]. Brain Res Rev 1995; 20: 91–127.

Parmeggiani PL, Morrison A, Drucker-Colin RR. McGinty D. Brain mechanisms of sleep: an overview of methodological issues. In: McGinty DJ, Drucker-Colin R, Morrison A, Parmeggiani PL, editors. Brain mechanisms of sleep. New York: Raven Press, 1985: 1–33.

Partiot A, Grafman J, Sadato N, Wachs J, Hallett M. Brain activation during the generation of non-emotional and emotional plans. Neuroreport 1995; 6: 1397–400.

Phillips DS, Denney DD, Robertson RT, Hicks LH, Thompson RF. Cortical projections of ascending nonspecific systems. Physiol Behav 1972; 8: 269–77.

Pompeiano O. The neurophysiological mechanisms of the postural and motor events during desynchronized sleep. [Review]. Res Publ Assoc Res Nerv Ment Dis 1967; 45: 351–423.

Porrino LJ, Esposito RU, Seeger TF, Crane AM, Pert A, Sokoloff L. Metabolic mapping of the brain during rewarding self-stimulation. Science 1984; 224: 306–9.

Powell TPS, Cowan WM. A study of thalamo-striate relations in the monkey. Brain 1956; 79: 364–90.

Ramsay SC, Murphy K, Shea SA, Friston KJ, Lammertsma AA, Clark JC, et al. Changes in global cerebral blood flow in humans: effect on regional cerebral blood flow during a neural activation task. J Physiol (Lond) 1993; 471: 521–34.

Rechtschaffen A, Kales A (Editors). A manual of standardized terminology, techniques and scoring system for sleep stages of human subjects. Bethesda (MD): U. S. National Institute of Neurological Diseases and Blindness, Neurological Information Network, 1968.

Reiman EM, Raichle ME, Robins E, Butler FK, Herscovitch P, Fox P, et al. The application of positron emission tomography to the study of panic disorder. Am J Psychiatry 1986; 143: 469–77.

Reivich M, Isaacs G, Evarts E, Kety S. The effect of slow wave sleep and REM sleep on regional cerebral blood flow in cats. J Neurochem 1968; 15: 301–6.

Richardson TL, Miller JJ, McLennan H. Mechanisms of excitation and inhibition in the nigrostriatal system. Brain Res 1977; 127: 219–34.

Robertson RT, Lynch GS, Thompson RF. Diencephalic distributions of ascending reticular systems. Brain Res 1973; 55: 309–22.

Robin ED, Whaley RD, Crump CH, Travis DM. Alveolar gas tensions, pulmonary ventilation and blood pH during physiologic sleep in normal subjects. J Clin Invest 1958; 37: 981–9.

Royce GJ, Bromley S, Gracco C, Beckstead RM. Thalamocortical connections of the rostral intralaminar nuclei: an autoradiographic analysis in the cat. J Comp Neurol 1989; 288: 555–82.

Royce GJ, Mourey RJ. Efferent connections of the centromedian and parafascicular thalamic nuclei: an autoradiographic investigation in the cat. J Comp Neurol 1985; 235: 277–300.

Rye DB, Wainer BH, Mesulam MM, Mufson EJ, Saper CB. Cortical projections arising from the basal forebrain: a study of cholinergic and non cholinergic components employing combined retrograde tracing and immunohistochemical localization of choline acetyltransferase. Neuroscience 1984; 13: 627–43.

Sadikot AF, Parent A, Francois C. The centre median and parafascicular thalamic nuclei project respectively to the sensorimotor and associative-limbic striatal territories in the squirrel monkey. Brain Res 1990; 510: 161–5.

Sakai K, Petitjean F, Jouvet M. Effects of ponto-mesencephalic lesions and electrical stimulation upon PGO waves and EMPs in unanesthetized cats. Electroencephalogr Clin Neurophysiol 1976; 41: 49–63.

Sarkadi A, Tram Anh DT, Nagy A, Tomka I. Activity of the corpus striatum of cats during natural sleep; a correlation analysis study. Acta Physiol Acad Sci Hung 1974; 45: 233–42.

Sasaki K. Electrophysiological studies on thalamo-cortical projections. [Review]. Int Anesthesiol Clin 1975; 13: 1–35.

Sasaki K, Staunton HP, Dieckmann G. Characteristic features of augmenting and recruiting responses in the cerebral cortex. Exp Neurol 1970; 26: 369–92.

Sayers A, Stille G. The caudate spindle during various sleep stages. Experientia 1972; 28: 282–4.

Scheibel ME, Scheibel AB. Structural organization of nonspecific thalamic nuclei and their projection toward cortex. Brain Res 1967; 6: 60–94.

Schneider JS. Functions of the basal ganglia: an overview. In: Schneider JS, Lidsky TI, editors. Basal ganglia and behavior: sensory aspects of motor functioning. Toronto: Hans Huber, 1987: 1–8.

Semba K. The cholinergic basal forebrain: a critical role in cortical arousal. In: Napier TC, Kalivas PW, Hanin I, editors. The basal forebrain. Anatomy to function. New York: Plenum Press, 1991: 197–218.

Siegel JM. Ponto-medullary interactions in the generation of REM sleep. In: McGinty DJ, Drucker-Colin R, Morrison A, Parmeggiani PL, editors. Brain mechanisms of sleep. New York: Raven Press, 1985: 157–74.

Smith C. Sleep states and learning: a review of the animal literature. [Review]. Neurosci Biobehav Rev 1985; 9: 157–68.

Snyder F. In: Madow L, Snow LH, editors. The psychodynamic implications of the physiological studies on dreams. Springfield (IL): Charles C. Thomas, 1970: 124–51.

Starzl TE, Magoun HW. Organization of the diffuse thalamic projection system. J Neurophysiol 1951; 14: 133–46.

Steriade M. Mechanisms underlying cortical activation: neuronal organization and properties of the midbrain reticular core and intralaminar thalamic nuclei. In: Pompeiano O, Ajmone Marsan C,

editors. Brain mechanisms of perceptual awareness and purposeful behavior. New York: Raven Press, 1981: 327–77.

Steriade M. Basic mechanisms of sleep generation. [Review]. Neurology 1992; 42(7 Suppl 6): 9–18.

Steriade M. Arousal: revisiting the reticular activating system [comment]. [Review]. Science 1996; 272: 225–6. Comment on: Science 1996; 272: 271–7.

Takahashi Y, Kipnis DM, Daughaday WH. Growth hormone secretion during sleep. J Clin Invest 1968; 47: 2079–90.

Talairach J, Tournoux P. Co-planar stereotaxic atlas of the human brain. Stuttgart: Thieme, 1988.

Velluti R, Yamuy J, Hadjez J, Monti JM. Spontaneous cerebellar nuclei PGO-like waves in natural paradoxical sleep and under reserpine. Electroencephalogr Clin Neurophysiol 1985; 60: 243–8.

Vertes RP. Brainstem control of the events of REM sleep. [Review]. Prog Neurobiol 1984; 22: 241–88.

Villablanca J. Permanent reduction in sleep after removal of cerebral cortex and striatum in cats. Brain Res 1972; 36: 463–8.

Vogt BA, Finch DM, Olson CR. Functional heterogeneity in cingulate cortex: the anterior executive and posterior evaluative regions. [Review]. Cereb Cortex 1992; 2: 435–43.

Williams HL, Hammack JT, Daly RL, Dement WC, Lubin A. Responses to auditory stimulation, sleep loss and the EEG stages of sleep. Electroencephalogr Clin Neurophysiol 1964; 16: 269–79.

Wilson CJ. Basal ganglia. In: Shepherd GM, editor. The synaptic organisation of the brain. 3rd ed. New York: Oxford University Press, 1990: 279–316.

Received January 21, 1997. Accepted February 28, 1997